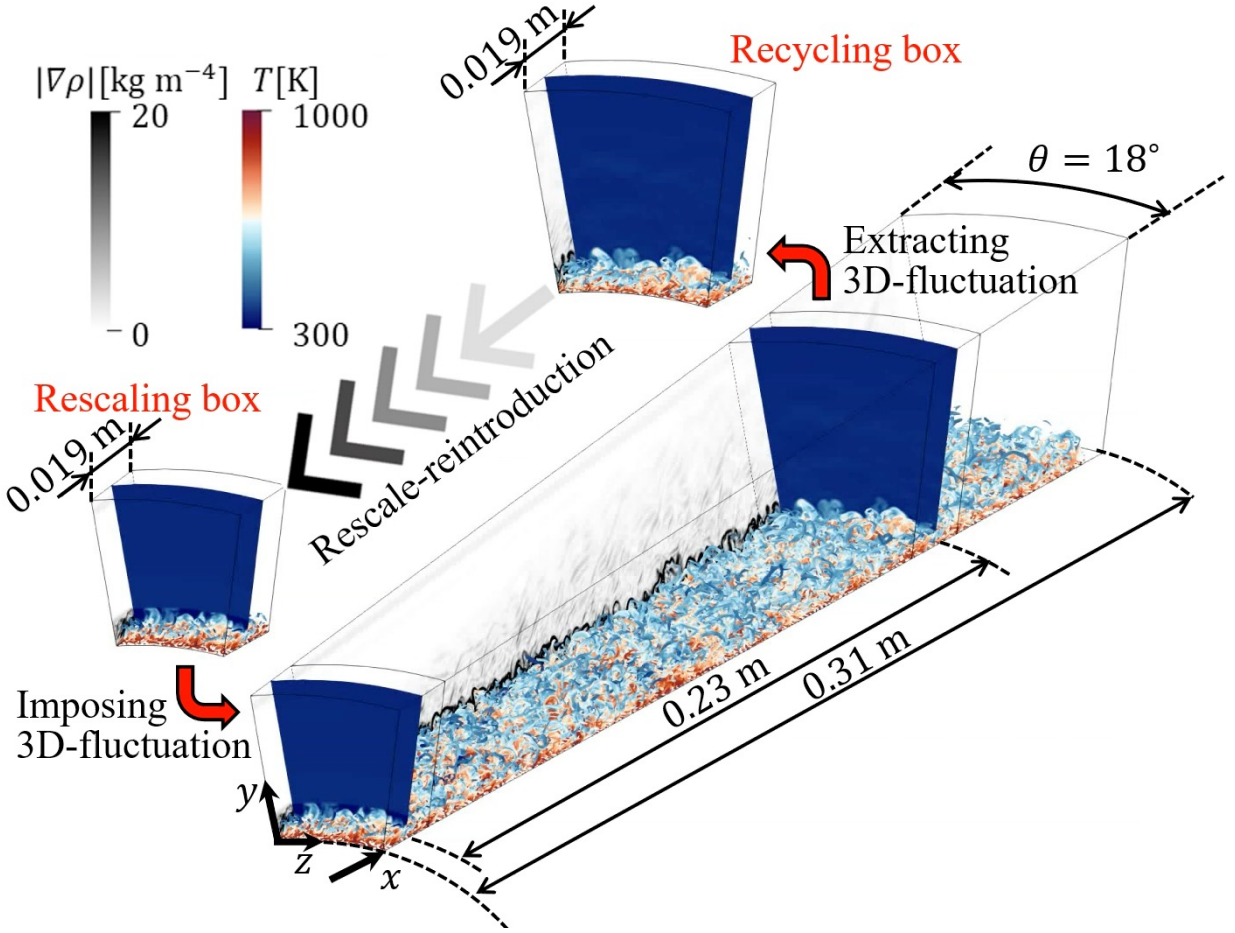
Sub-filter scale shear stress deficit in hypersonic wall-bounded turbulence and its implications for large-eddy simulation

Takahiko Toki

School of Mechanical Engineering

Purdue University, IN USA



FY21 ONR MURI Turbulent/Chemistry
Grant No: N00014-21-1-2475
FY23 ONR Core Program
Grant No: N00014-23-1-2560

Advanced Modeling & Simulation (AMS) Seminar Series

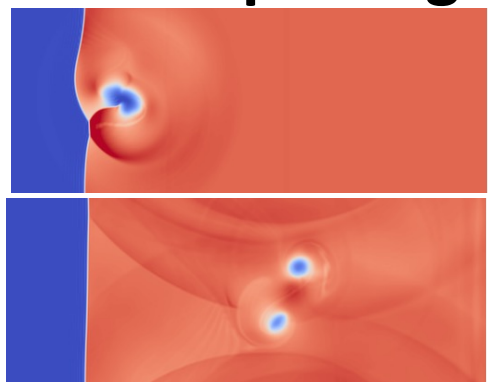
NASA Ames Research Center, April 2nd, 2026

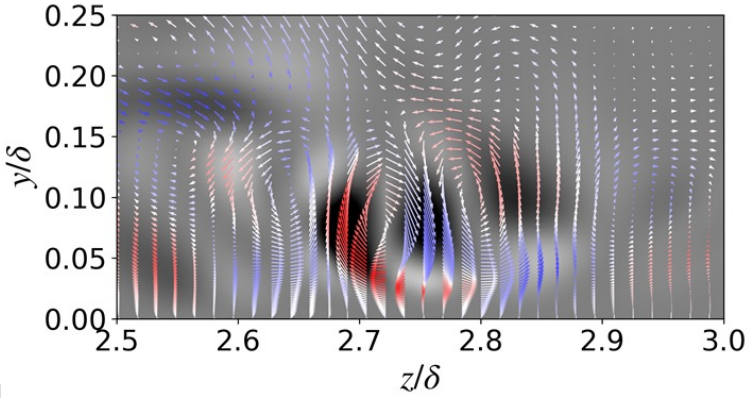
Introduction

Flow physics in hypersonic flights

PURDUE UNIVERSITY

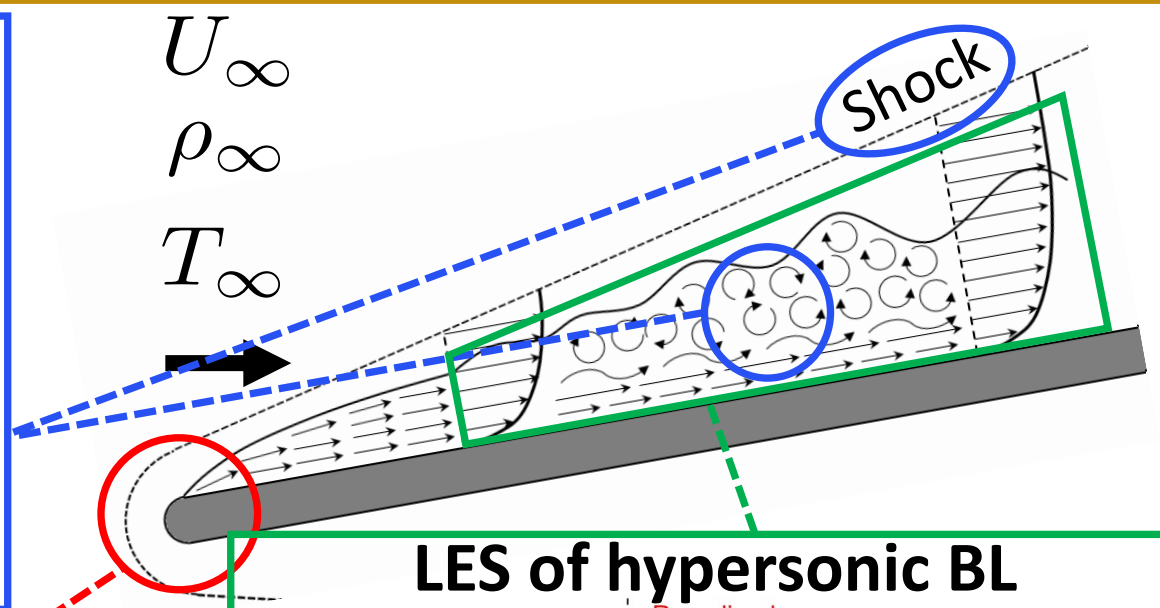
Shock capturing and LES modelling



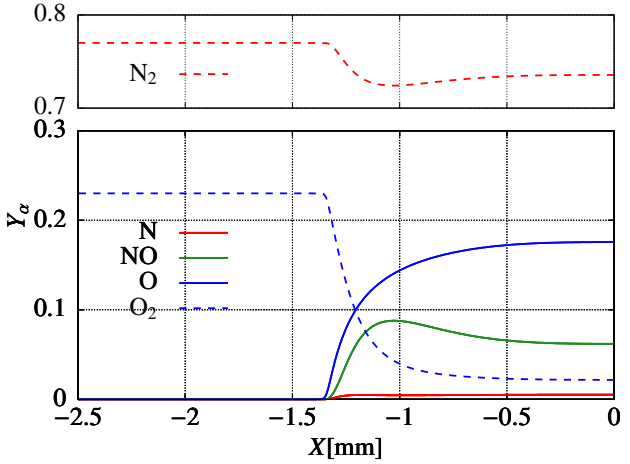


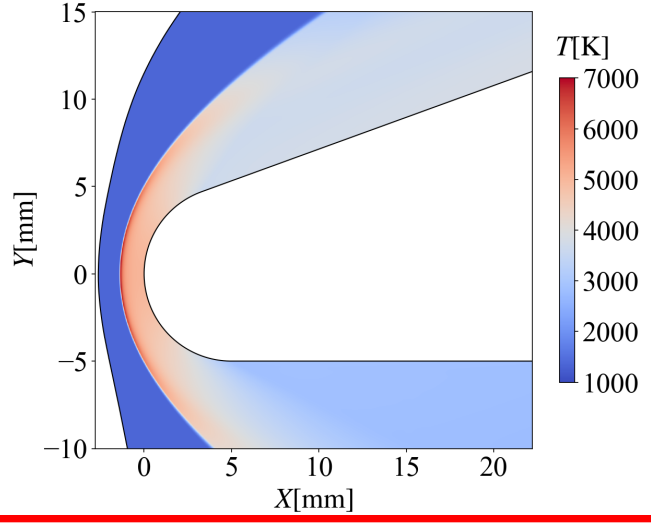
Lucarelli, Toki, & Scalo, in prep for JCP

Toki & Scalo, JFM 2024



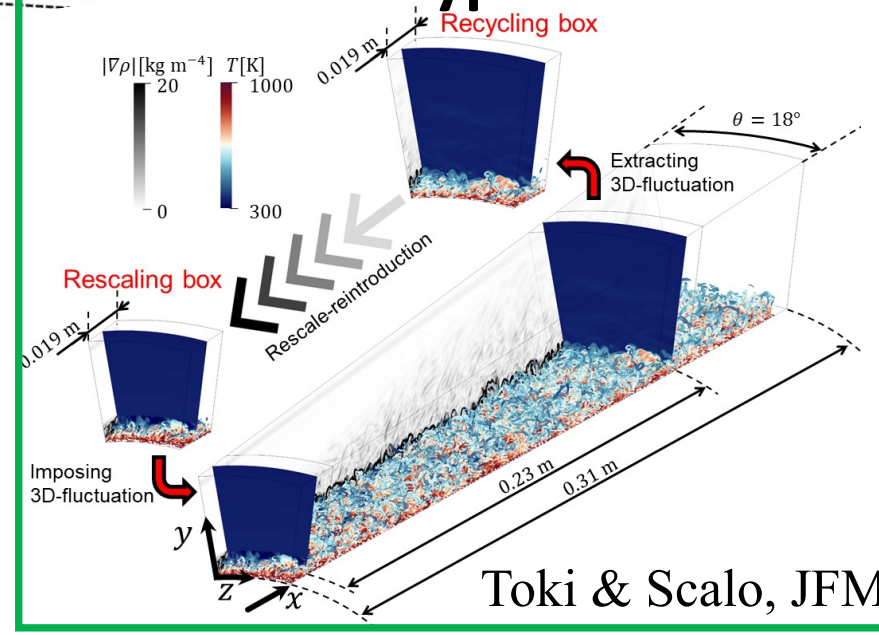
Aerodynamic heating and aerothermochemistry





Toki & Scalo, in prep for JFM

LES of hypersonic BL

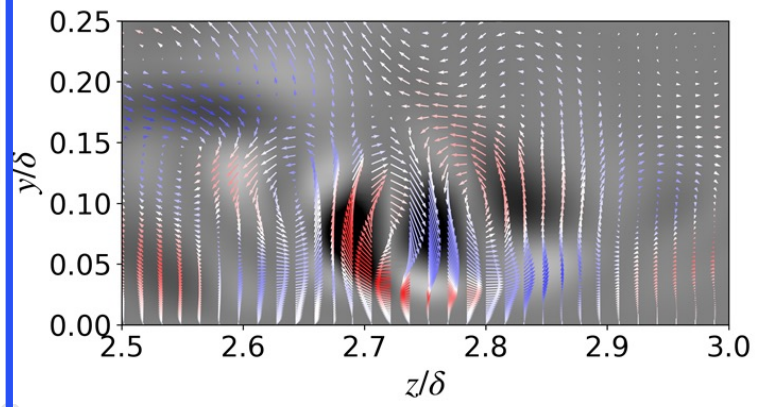


Toki & Scalo, JFM 2025

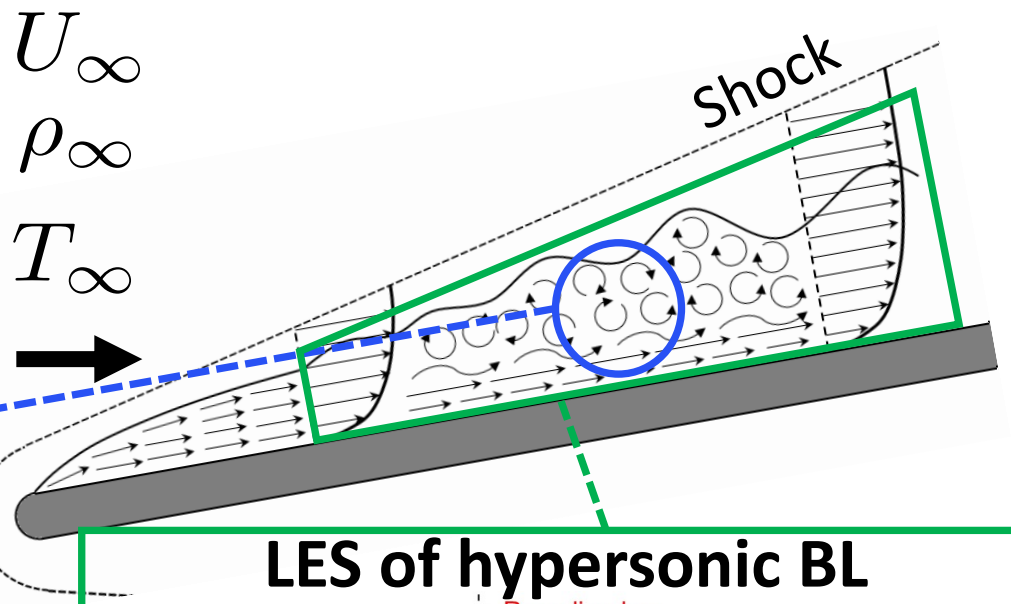
Flow physics in hypersonic flights

PURDUE UNIVERSITY

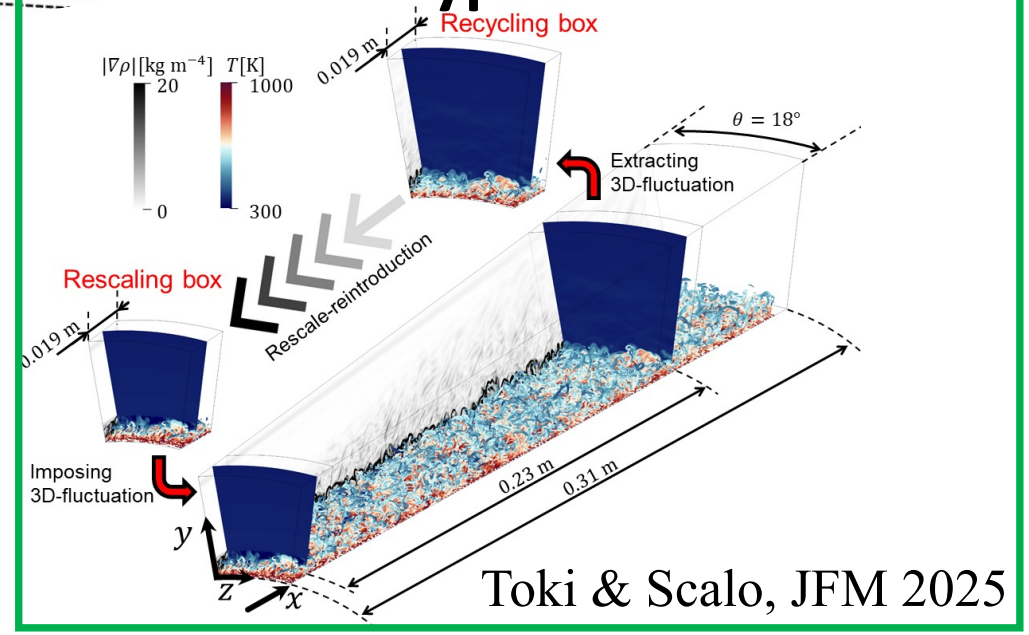
LES modelling



Toki & Scalo, JFM 2024



LES of hypersonic BL



Toki & Scalo, JFM 2025

Shock capturing and

Lucarelli, Toki & Scalo, in prep for JCP

Aerodynamic heating and aerothermochemistry

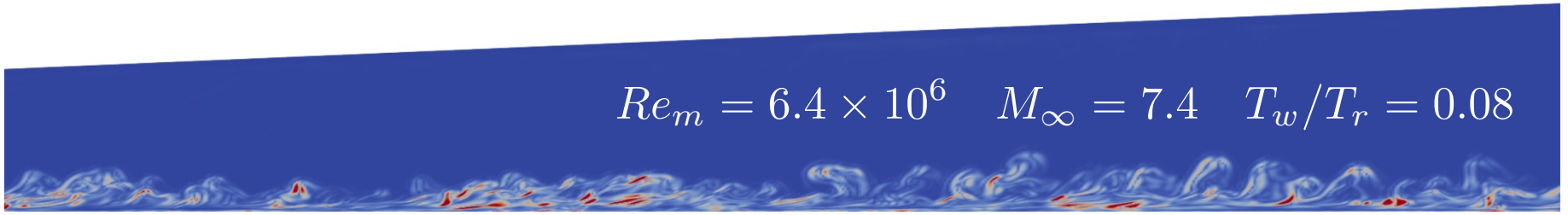
Toki & Scalo, in prep for JFM

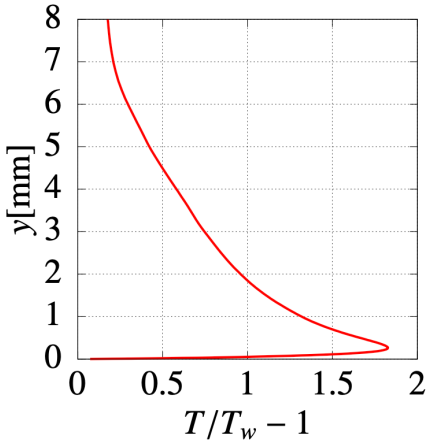
Motivation for hypersonic LES studies

PURDUE UNIVERSITY

Limiting factors in simulating attached hypersonic boundary layers

- ❑ Wall-resolved LES (WRLES) shares similar time-steps with Direct-Numerical Simulation (DNS)
- ❑ Subsonic and Supersonic simulations are limited by acoustic CFL at the first grid point from the wall.
- ❑ Hypersonic ones are limited by thermal conductivity CFL at peak temperature location (y* = 5- 12)



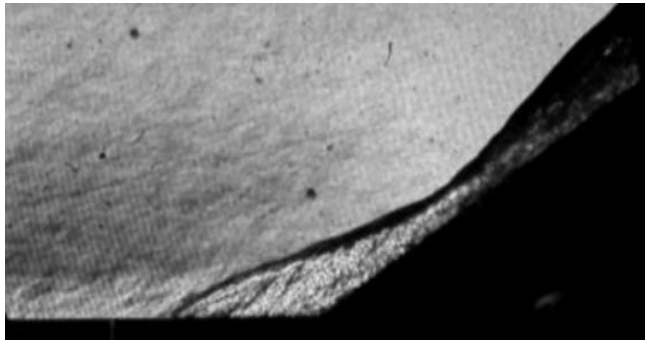


Shock wave and boundary layer interaction

- ❑ Large-scale low-frequency unsteadiness requires Wall-modeled LES (WMLES)

Case	M6			M8		
Method	DNS	LES	WMLES	DNS	LES	WMLES
CPU hours	92,160	6,910	35	92,160	5,760	29

Estimate for current Couette flow calculations @ CUBRC conditions



CUBRC, 2014

Favre-Filtered Navier-Stokes Equations

Closure is based on Favre-filtered compressible equations

$$\check{f} = \frac{\overline{\rho f}}{\overline{\rho}}.$$

$$\frac{\partial \overline{\rho}}{\partial t} + \frac{\partial \overline{\rho}\check{u}_j}{\partial x_j} = 0,$$

$$\frac{\partial \overline{\rho}\check{u}_i}{\partial t} + \frac{\partial \overline{\rho}\check{u}_i\check{u}_j}{\partial x_j} = -\frac{\partial \overline{p}}{\partial x_i} + \frac{\partial \mu \check{\sigma}_{ij}}{\partial x_j} - \frac{\partial \overline{\rho}\tau_{ij}}{\partial x_j},$$

$$\frac{\partial \overline{E}}{\partial t} + \frac{\partial (\overline{E}+\overline{p})\check{u}_j}{\partial x_j} = \frac{\partial}{\partial x_j}\left(k\frac{\partial \check{T}}{\partial x_j}\right) + \frac{\partial \mu \check{\sigma}_{ij}\check{u}_i}{\partial x_j} - \frac{\partial \overline{\rho} C_p q_j}{\partial x_j} - \frac{\partial}{\partial x_j}\left(\frac{1}{2}\overline{\rho}\pi_j\right) + \mu\epsilon,$$

$$\frac{\overline{p}}{\gamma - 1} = \overline{E} - \frac{1}{2}\overline{\rho}\check{u}_i\check{u}_i - \frac{1}{2}\overline{\rho}\tau_{ii}.$$

Unclosed terms

$$\tau_{ij} = \widetilde{u_i u_j} - \check{u}_i\check{u}_j,$$

$$q_j = \widetilde{T u_j} - \check{T}\check{u}_j,$$

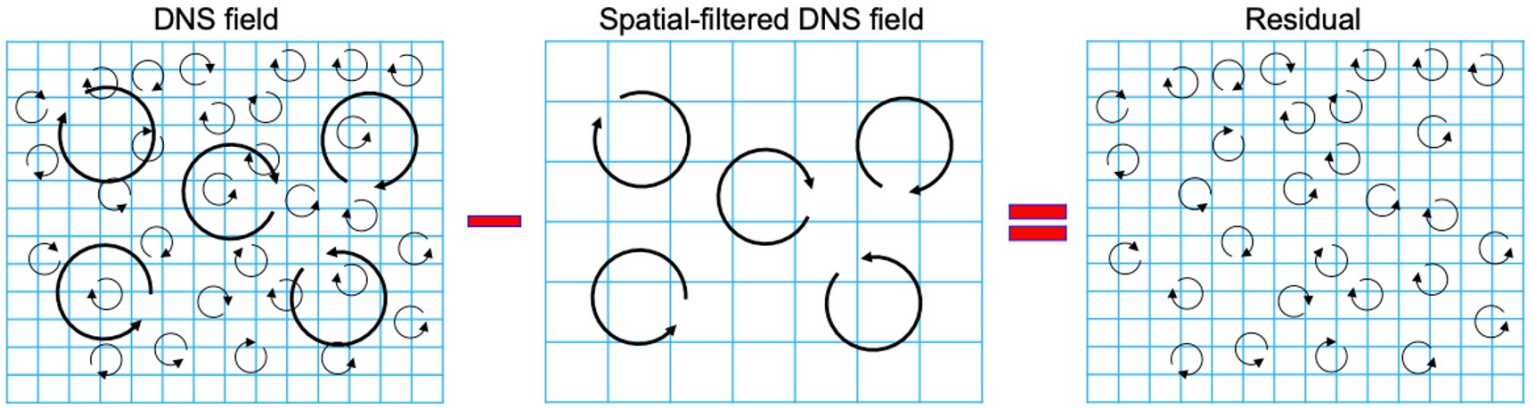
$$\pi_j = \widetilde{u_k u_k u_j} - \check{u}_k\check{u}_k\check{u}_j$$

$$\epsilon = \frac{\partial \overline{\sigma_{ij}u_i}}{\partial x_j} - \frac{\partial \check{\sigma}_{ij}\check{u}_i}{\partial x_j}.$$

Exact and *a priori* sub-filter scale (SFS) analyses

PURDUE UNIVERSITY

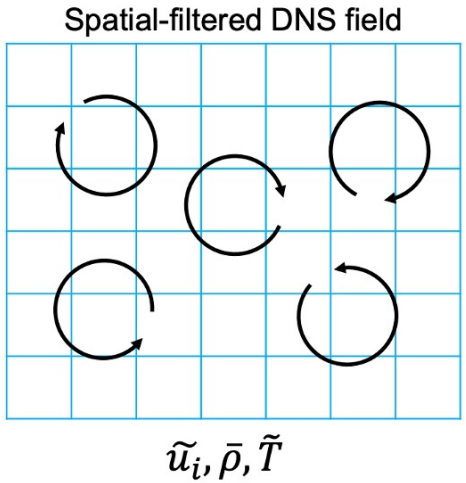
Exact SFS extraction



$$\tau_{ij}^{SFS} = \widetilde{u_i u_j} - \tilde{u}_i \tilde{u}_j$$

$$q_j^{SFS} = \widetilde{T u_j} - \tilde{T} \tilde{u}_j$$

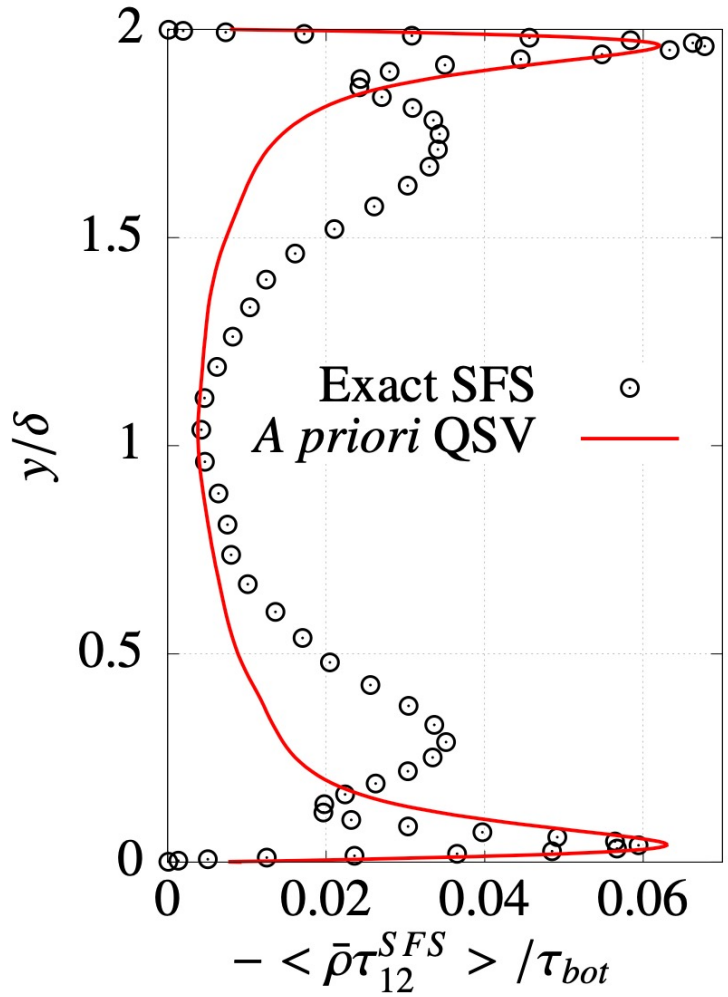
A priori analysis



SFS Model (QSV)

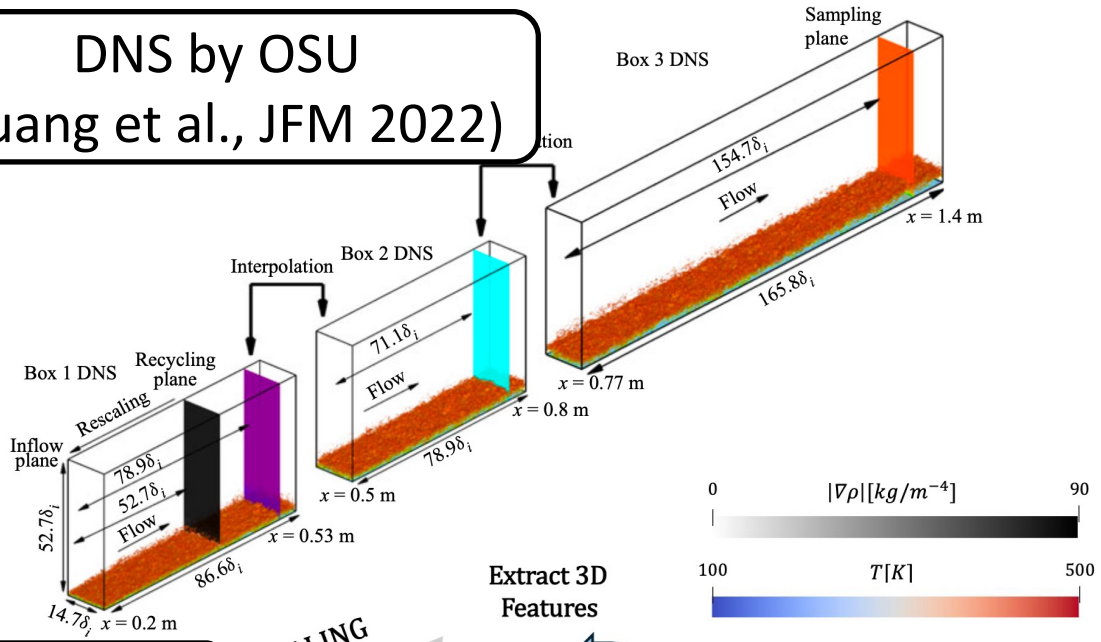
$$\tau_{ij} = -\frac{1}{2} C_{\tau_{ij}} \left[D_{ij} \left[\frac{\partial \tilde{u}_i}{\partial x_j} \right] * \left(1 - G_{qsv,ij}\right) + D_{ji} \left[\frac{\partial \tilde{u}_j}{\partial x_i} \right] * \left(1 - G_{qsv,ji}\right) \right]$$

$$q_j = -C_q \left[D_{jj} \left[\frac{\partial \tilde{T}}{\partial x_j} \right] * \left(1 - G_{qsv,jj}\right) \right]$$

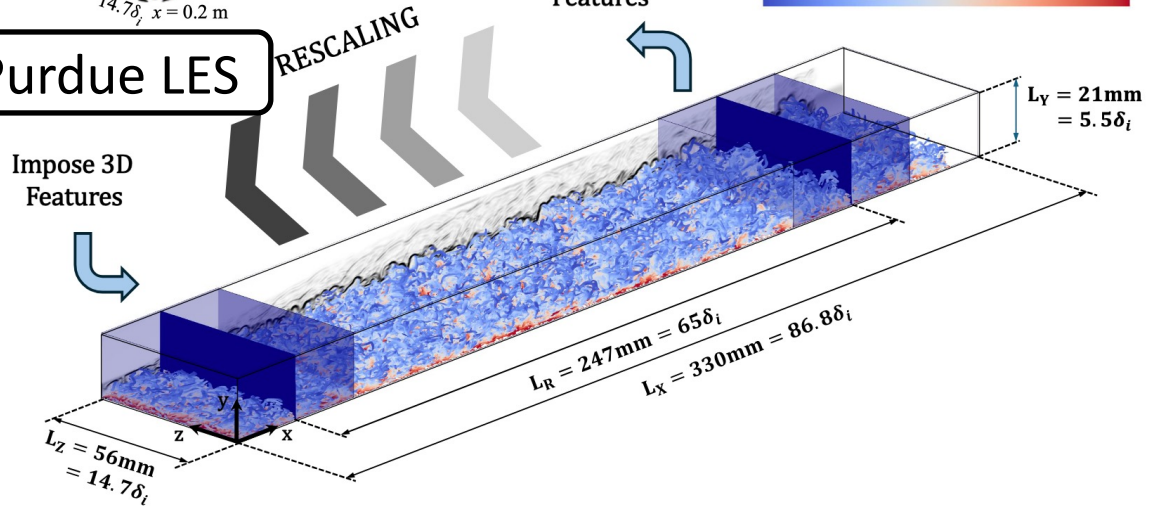


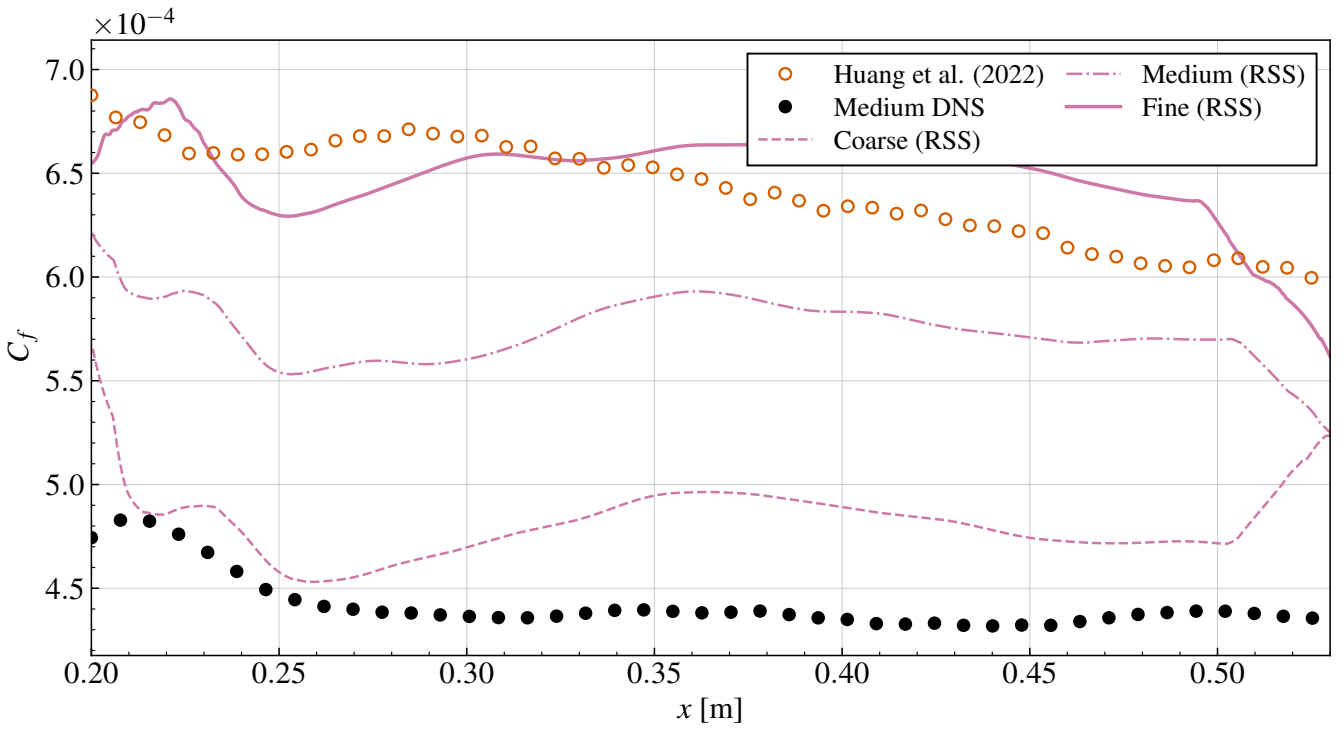
A posteriori LES

DNS by OSU
(Huang et al., JFM 2022)



Purdue LES





- Conduct LES of a certain flow field, where several validation datasets are available.
  - ➢ Evaluate the performance of the developed LES models.

Nicola Lucarelli, Takahiko Toki, Biswaranjan Pati, and Carlo Scalo, Residual Scale Sensing (RSS): A Unified Shock-Capturing, LES Model From Incompressible to Hypersonic Applications, Journal of Computational Physics, in preparation.

A posteriori LES of a hypersonic conical boundary layer

Takahiko Toki, Victor C.B. Sousa, Yongkai Chen, Giannino Ponchio Camillo, Alexander Wagner and Carlo Scalo, "Large-eddy simulations of conical hypersonic turbulent boundary layers over cooled walls via volumetric rescaling method," *Journal of Fluid Mechanics*, Vol. 1003, A28, 2025.

Reference experiment

HEG wind tunnel: DLR, *Journal of large-scale research facilities* Vol.4, A133

Geometry: 7° half-angle cone

Mach number: 7.4

Re number: 1.5-9.8 million [1/m]

Temperature ratio: $T_w/T_r \approx 0.1$



LESs of hypersonic boundary layers at the HEG condition are carried out .

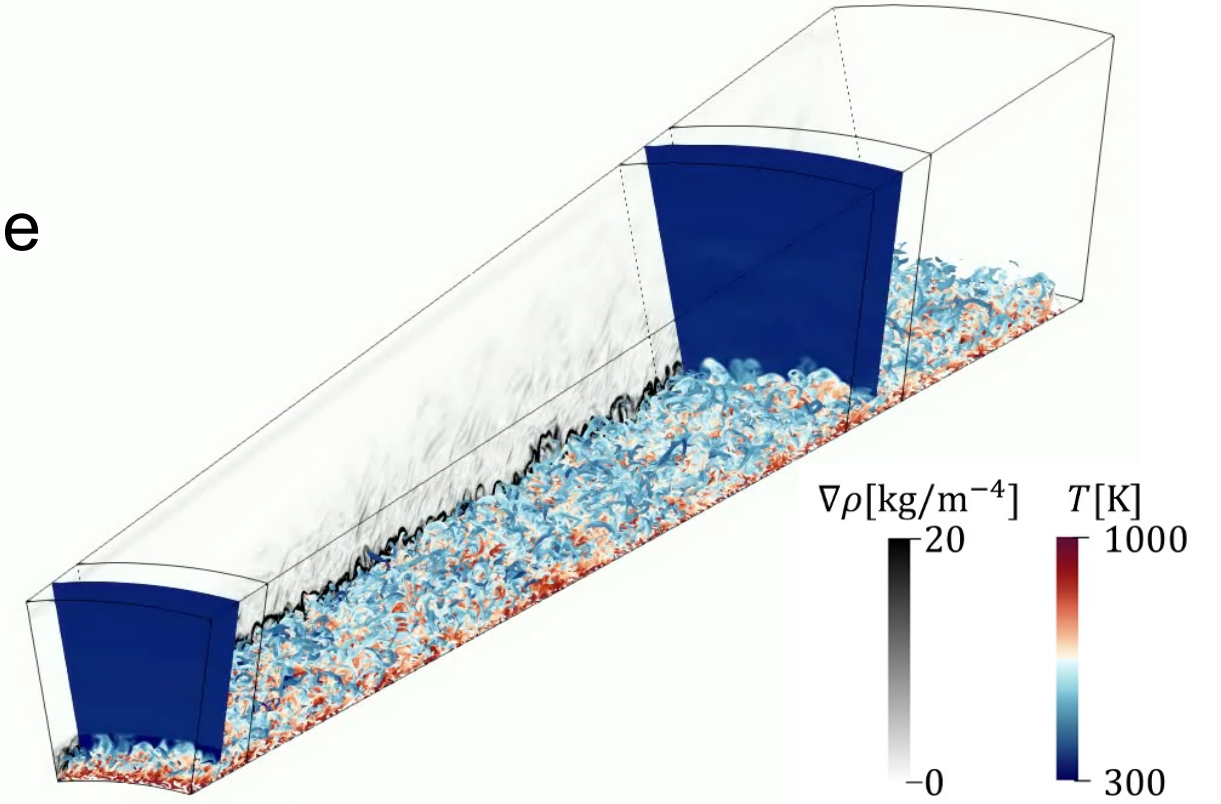
Re_m: $4.1\times10^6[\mathrm{m}^{-1}]$

u_∞: $2422[\mathrm{ms}^{-1}]$

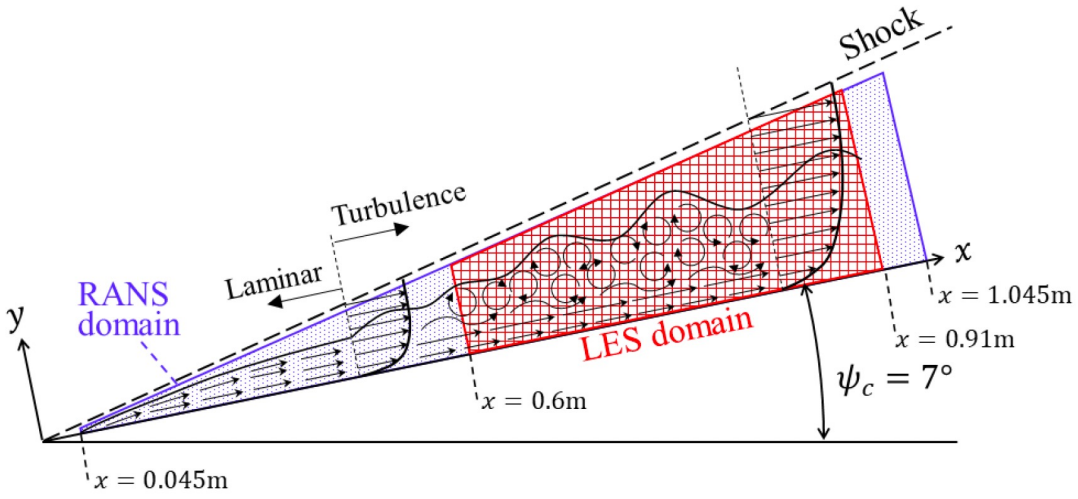
T_∞: $268[\mathrm{K}]$

p_∞: $2129[\mathrm{Pa}]$

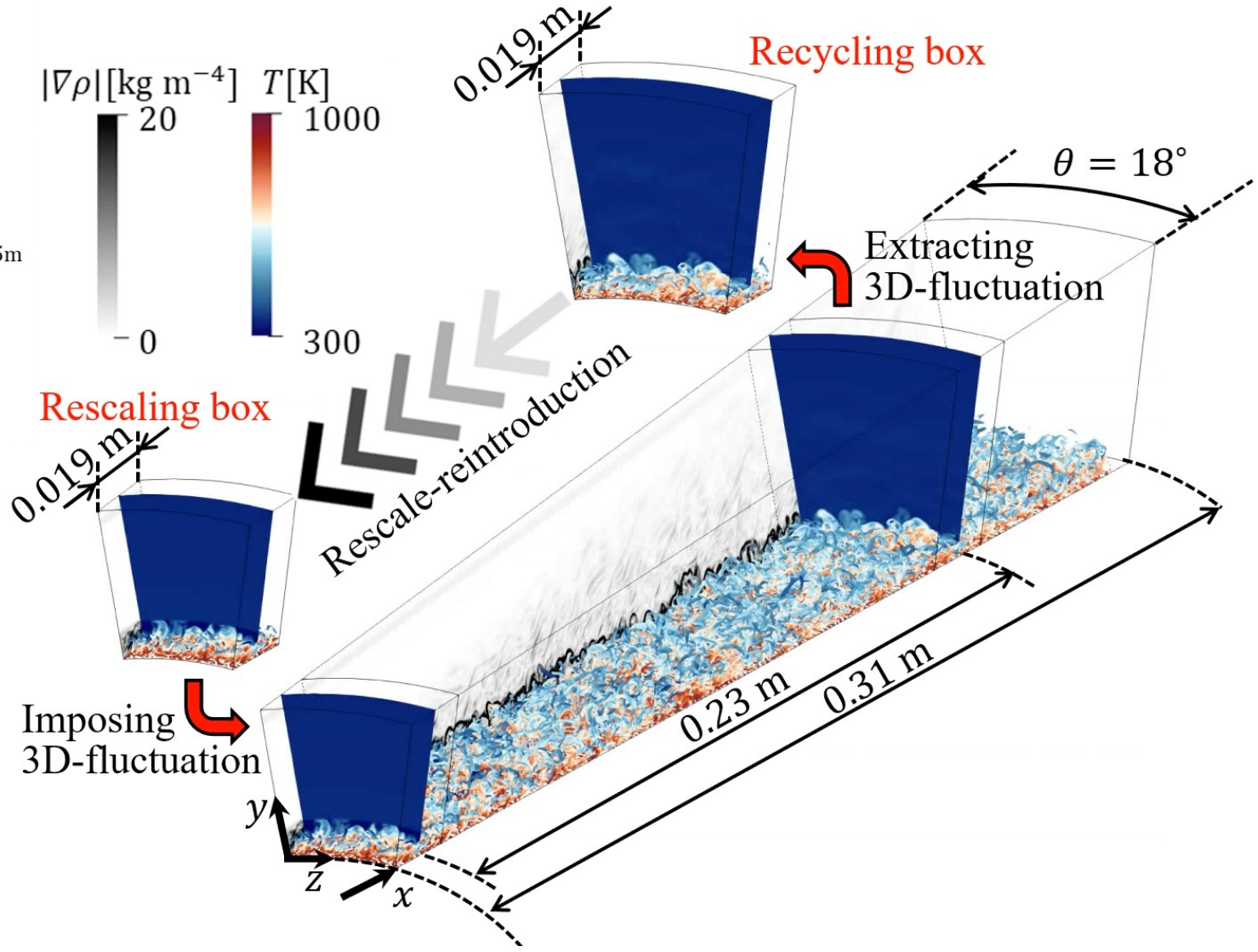
M_∞: 7.4



Computational domain & volumetric rescaling



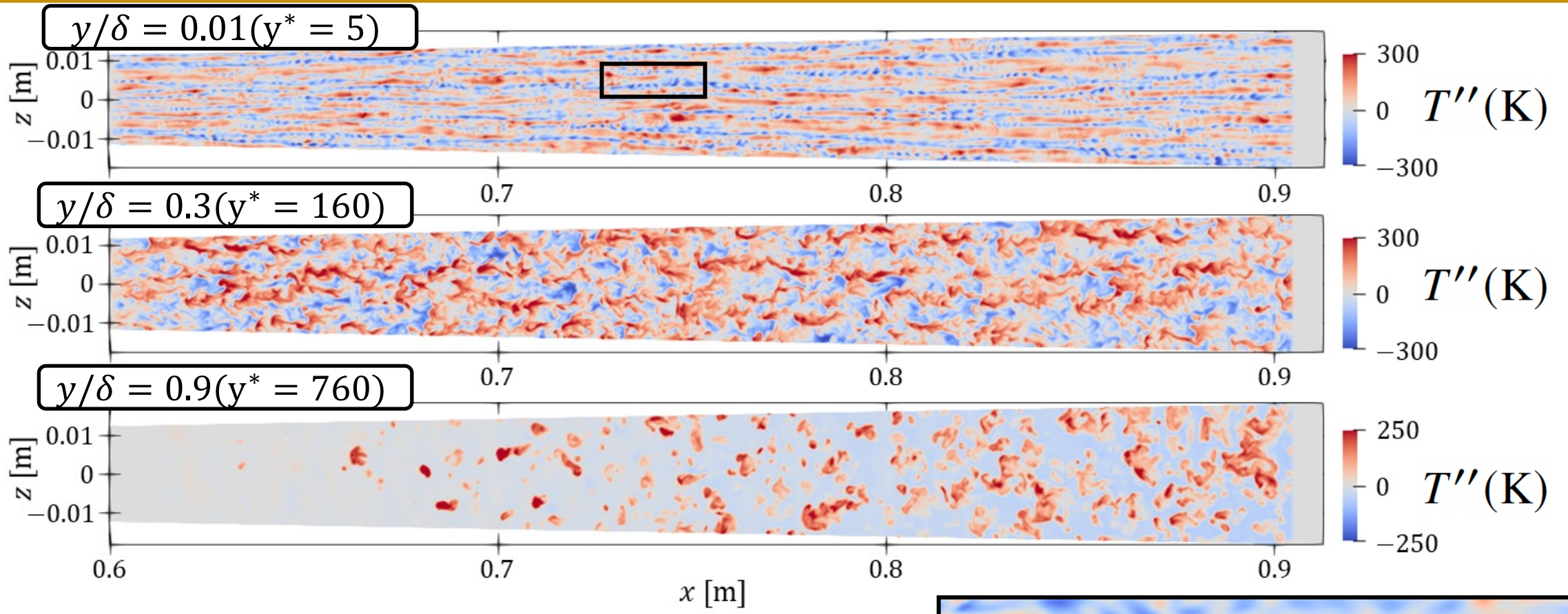
- Mean flow properties at the inlet are given by RANS.
- 3D structures of fluctuations are recycled at the inlet.
- The distance for the recycling region is $L_x = 0.23\ \mathrm{m} \approx 51\delta_{99}$



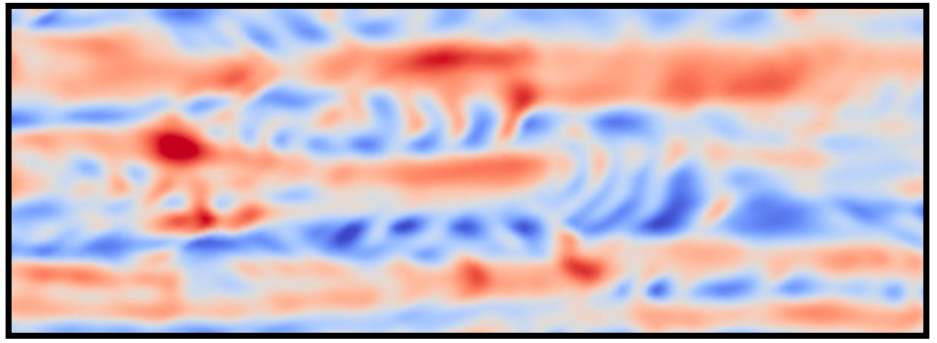
Numerical methods

Governing equations:	Favre-filtered compressible Navier-Stokes equations
Solver:	6th-order compact finite difference code (Nagarajan et al., 2003)
Turbulence closure:	Quasi-Spectral Viscosity (QSV) approach (Sousa & Scalo, 2022)
Shock capturing:	Quasi-Spectral Viscosity (QSV) approach (Sousa & Scalo, 2022)
Time integration:	Strong Stability Preserving (SSP) Runge-Kutta (Gottlieb, 2005)
Spatial filter:	6th-order compact filter with $\alpha = 0.495$ (Lele, 1992)

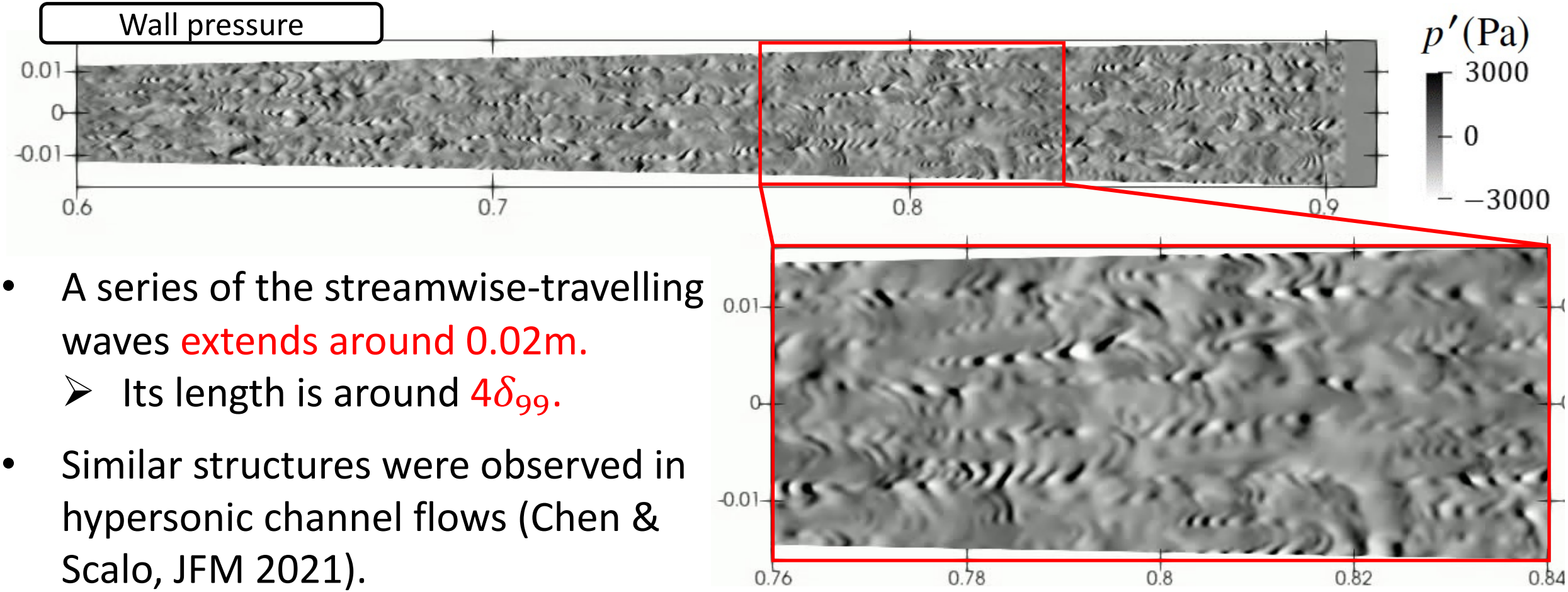
Flow structures in the wall-parallel plane



- Structures largely vary in the wall normal direction.
- Fine streaky structures are observed near the wall.
  - ➢ Strong fluctuations in low temperature streaks.



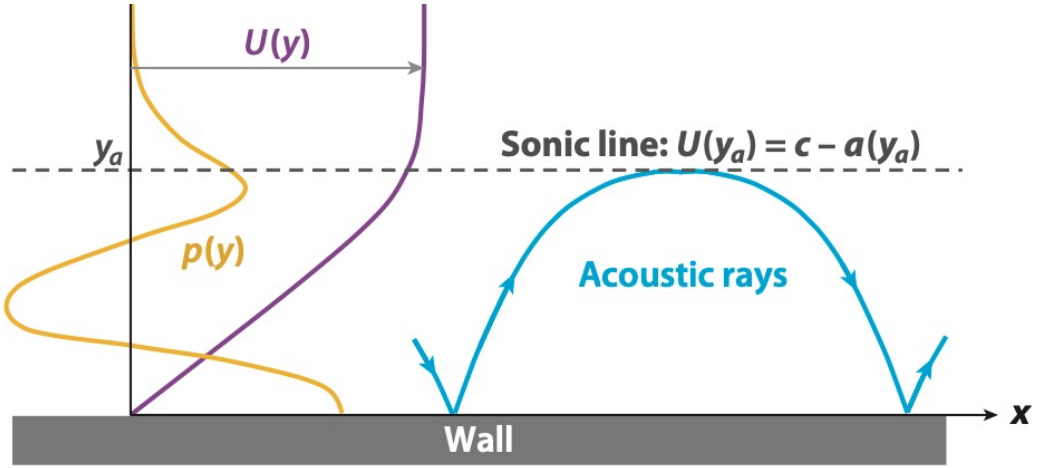
Streamwise-travelling wave (Trapped wave)



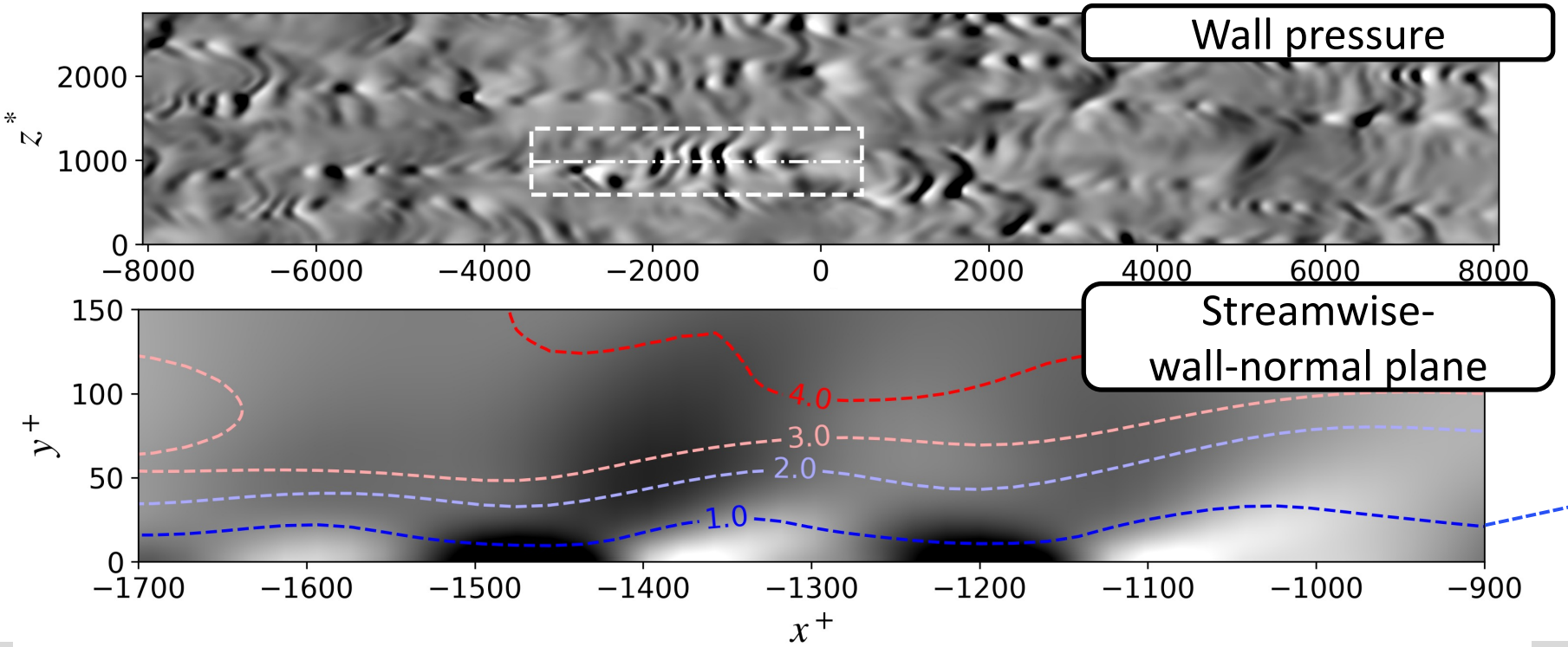
- A series of the streamwise-travelling waves extends around 0.02m.
  - ➢ Its length is around $4\delta_{99}$.
- Similar structures were observed in hypersonic channel flows (Chen & Scalo, JFM 2021).
  - ➢ Similar to second-mode instabilities in laminar flows.

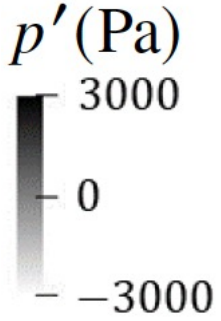
Streamwise-travelling wave (Trapped wave)

- A sonic line traps strong pressure fluctuations.
- Strong fluctuations extend to the line of Mach 1.0 and do not cross the line of Mach 2.0.
  - ➢ Same mechanism as the second-mode instability in the laminar



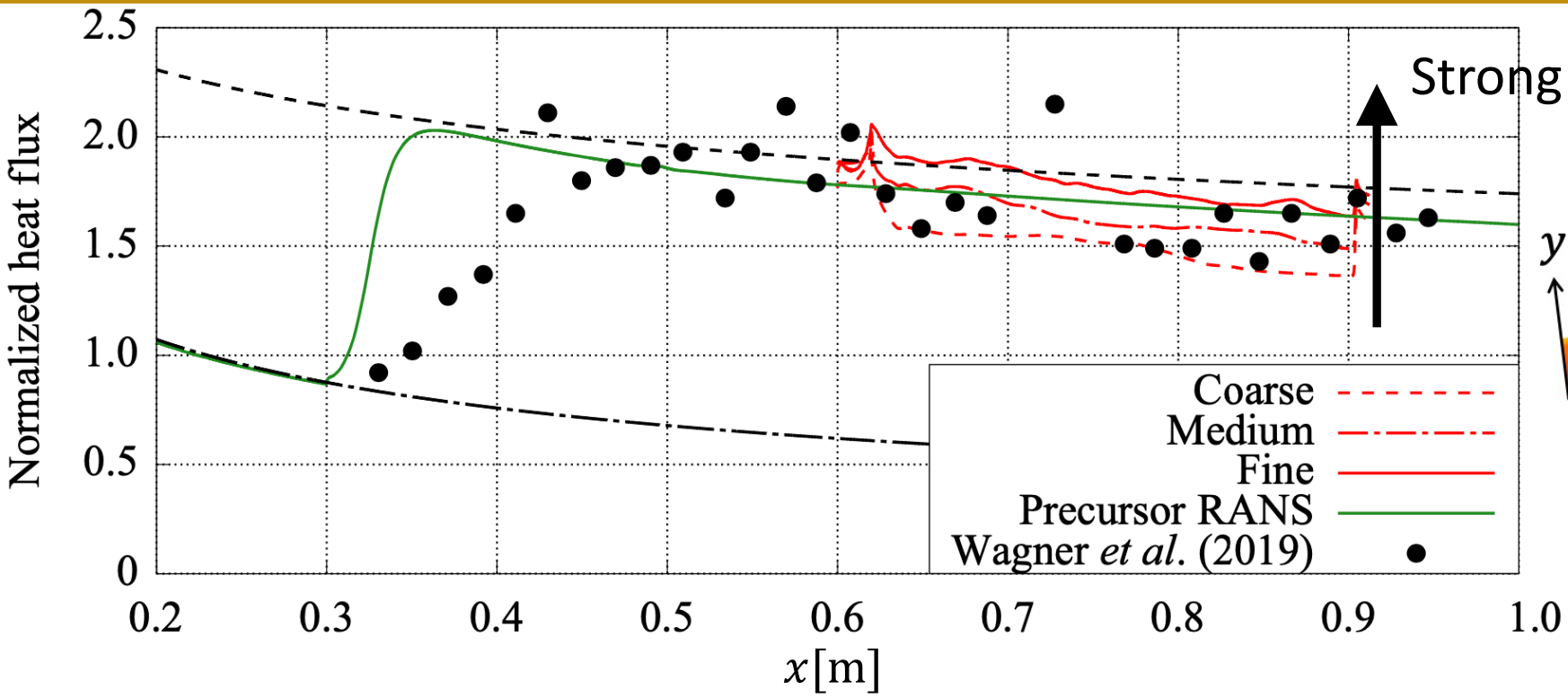
Fedorov, Annu. Rev. Fluid, 2011



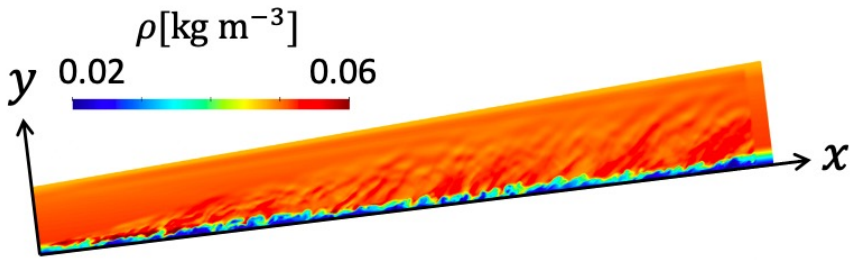


Sonic line
$M = 1.0$

Grid sensitivity for heat flux

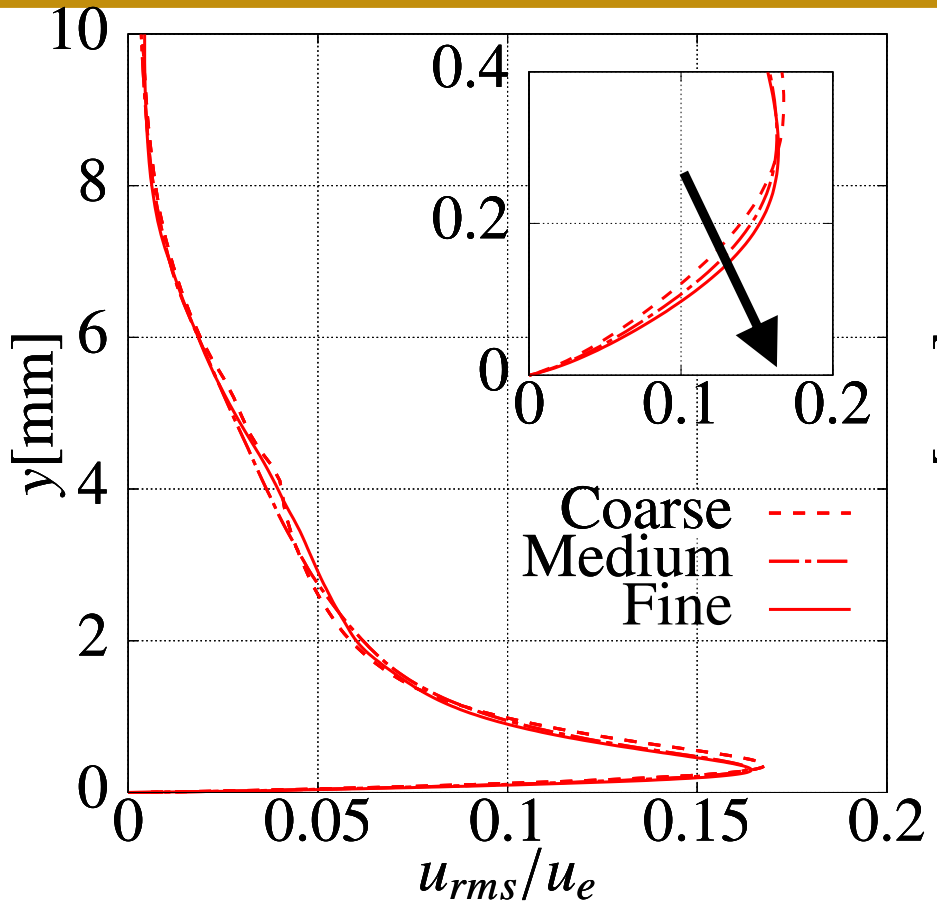


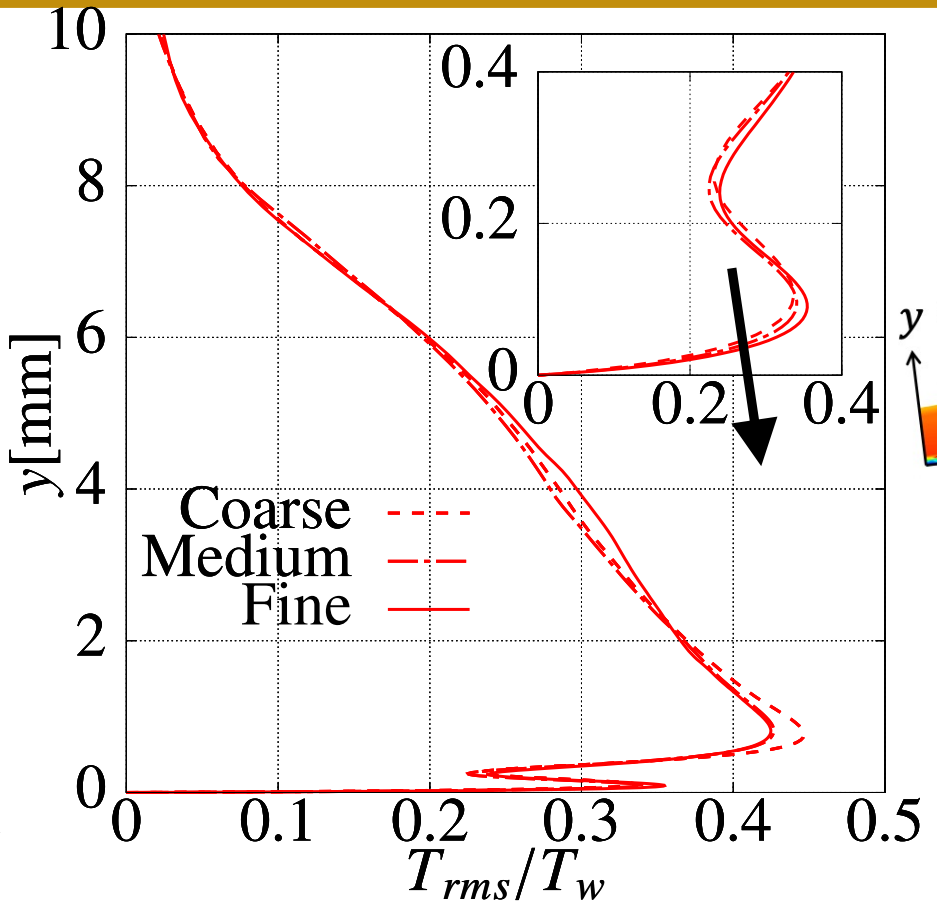
Strong grid sensitivity

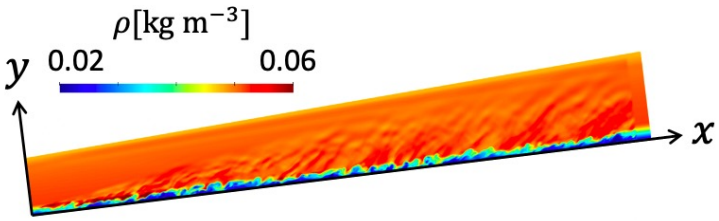


- The LES wall heat flux values are comparable with the experiment.
  - ➢ The current LES is able to discuss qualitative flow physics.
- Wall heat flux increases as the mesh is refined.
  - ➢ The current LES cannot provide a quantitative prediction of wall heat flux.

Grid sensitivity for fluctuations







RMSs are normalized by freestream velocity and wall temperature.

- Fluctuations are almost identical between the different meshes.
- Fluctuations differ only near the wall (viscous sublayer to buffer region).
  - ➢ Understanding of near-wall turbulence is important for the improvement of LES.

DNS of wall-bounded are carried out to investigate the near-wall SFS turbulence

Detailed analyses of SFS terms

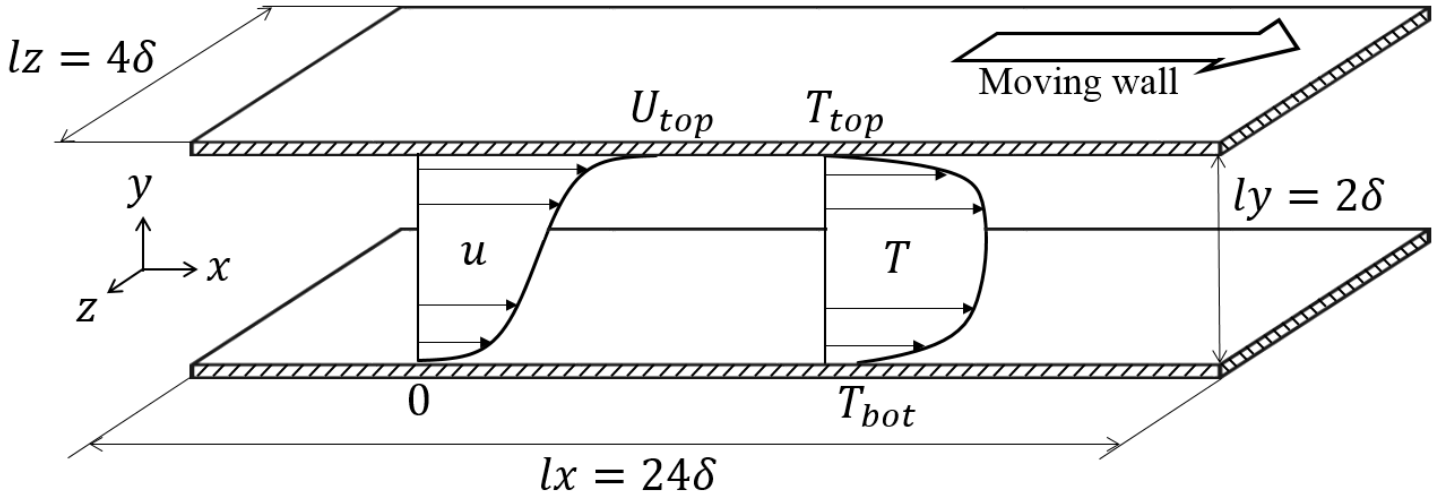
Takahiko Toki, Victor C. B. Sousa, Yongkai Chen and Carlo Scalo, "Sub-filter-scale (SFS) shear stress analysis in hypersonic turbulent Couette flow," *Journal of Fluid Mechanics*, Vol. 984, A53, 2024.

Computational configuration and conditions

PURDUE UNIVERSITY

Objective: *exact SFS analysis* from DNS of hypersonic Couette flow

Hypersonic turbulent Couette flow



Temperature:

$$T_{bot} = 300\ \mathrm{K}$$
$$T_{top} = 224\ \mathrm{K}$$

Velocity:

$$U_{top} = 1800 - 2400\ \mathrm{m/s}$$
$$Ma_{\mathrm{top}} = 6 - 8$$

Reynolds number:

$$620 \le Re_\tau \le 710\ ; Re_\tau \equiv u_\tau \delta/\nu,\ u_\tau \equiv \sqrt{\tau_{bot}/\rho}$$
$$210 \le Re_\tau^* \le 280\ ; Re_\tau^* \equiv u_\tau^* \delta/\nu_{center},\ u_\tau^* \equiv \sqrt{\tau_{bot}/\rho_{center}}$$

δ; half width of the channel, τ_{bot}; wall shear stress

Numerical methods

PURDUE UNIVERSITY

Computational schemes

Governing equations: 3D fully compressible Navier-Stokes equations

Solver: 6th-order compact finite difference code (Nagarajan et al., 2003)
+ 6th-order compact filter with $\alpha = 0.495$ (Lele, 1992)

Time integration: Strong Stability Preserving (SSP) Runge-Kutta (Gottlieb, 2005)

Analysis for SFS stress

Spatial filter: Sharp cutoff filter in streamwise and spanwise directions

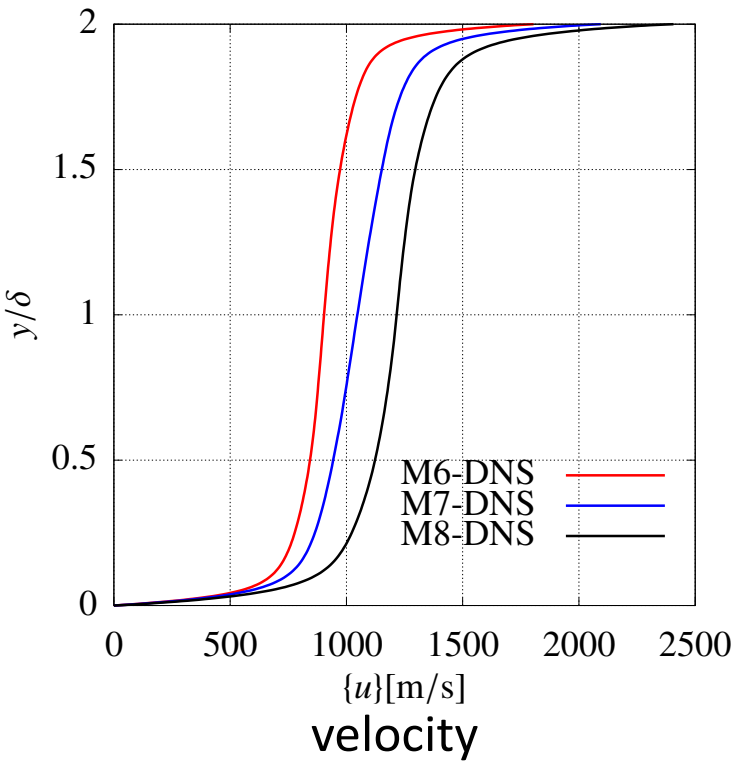
Filter widths: $\overline{\Delta} = 4\Delta x_i$ and $\overline{\Delta} = 8\Delta x_i$ (We mainly tested two filter widths)

$$\frac{\partial \overline{\rho}\widetilde{u_j}}{\partial t} + \frac{\partial \overline{\rho}\widetilde{u_j}\widetilde{u_j}}{\partial x_j} = -\frac{\partial \overline{p}}{\partial x_i} + \frac{\partial \overline{\sigma_{ij}}}{\partial x_j} - \boxed{\frac{\overline{\rho}\tau_{ij}}{\partial x_j}}$$

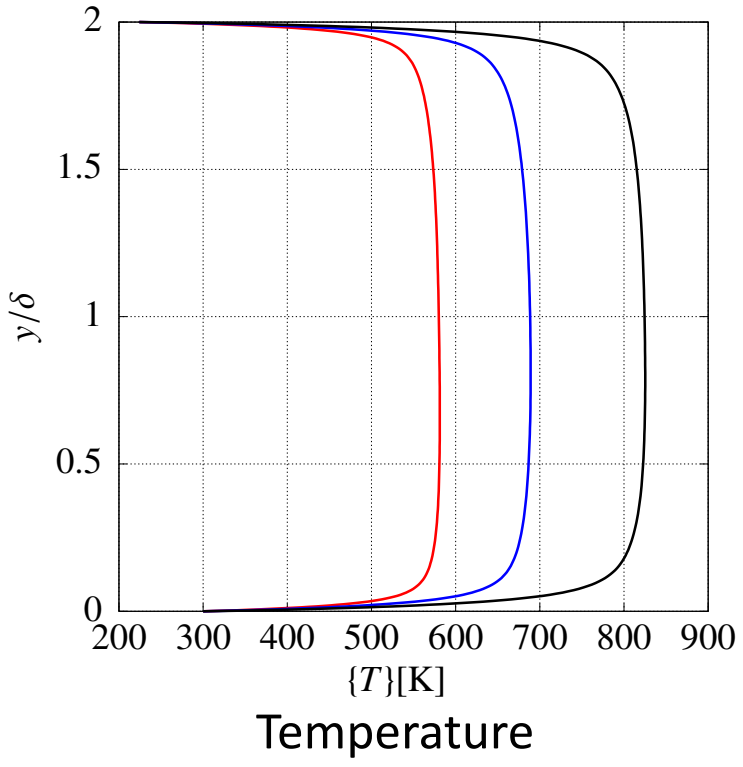
SFS stress: $\tau_{ij} = \widetilde{u_i u_j} - \widetilde{u_i}\widetilde{u_j}$

$\overline{(\cdot)}$: Spatial filter, $\widetilde{(\cdot)}$: Favre spatial filter

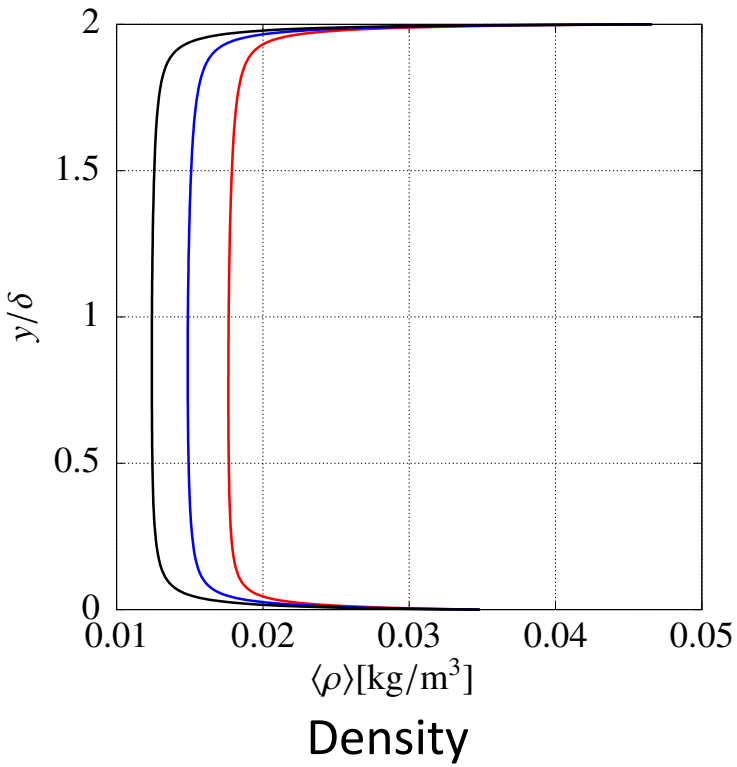
Mean profiles



velocity

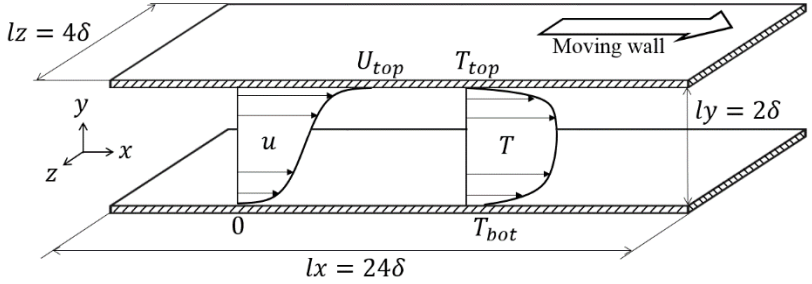


Temperature

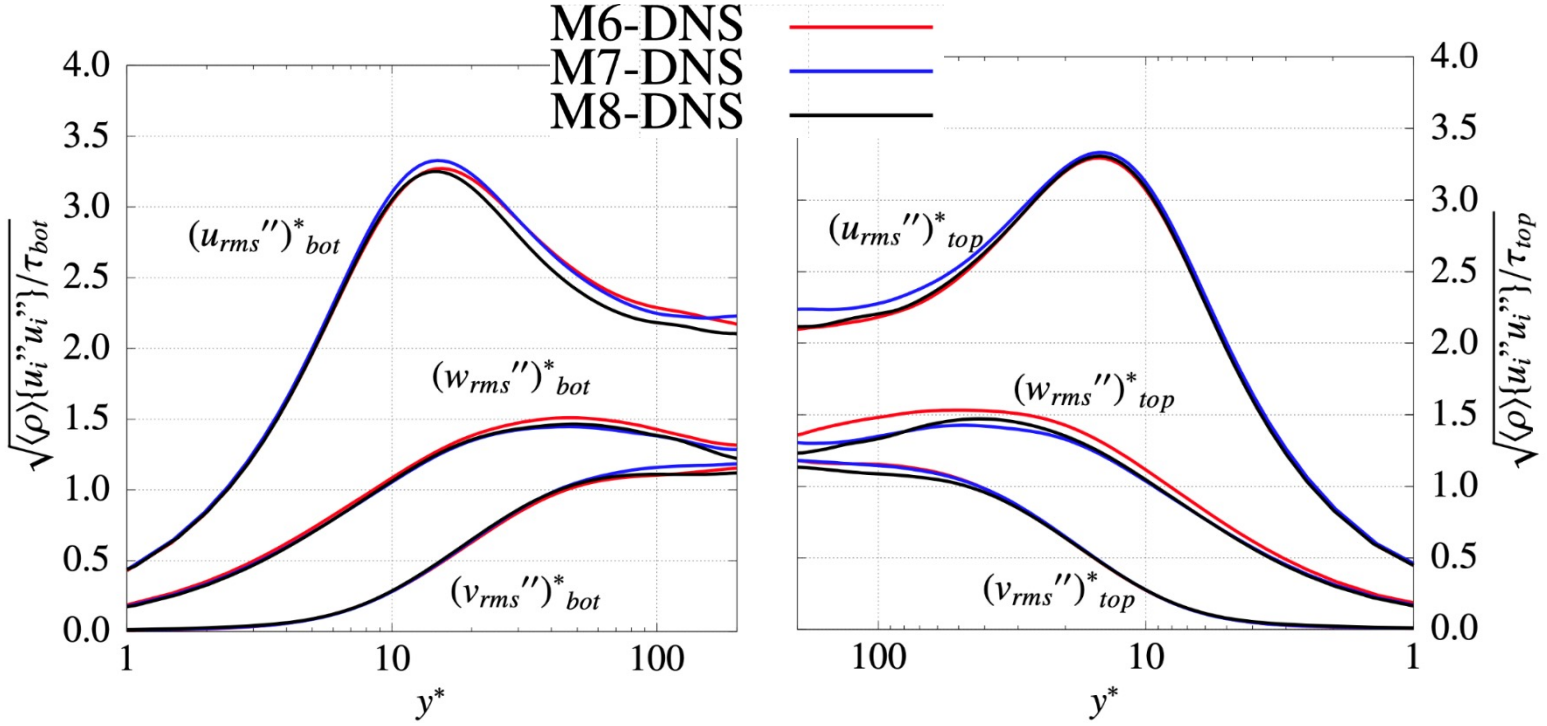


Density

- Temperature increases with increase in Mach number
- Density decreases with increase in Mach number
  - Fluid properties depend on Mach number
  - Fluid properties are largely different between the cases

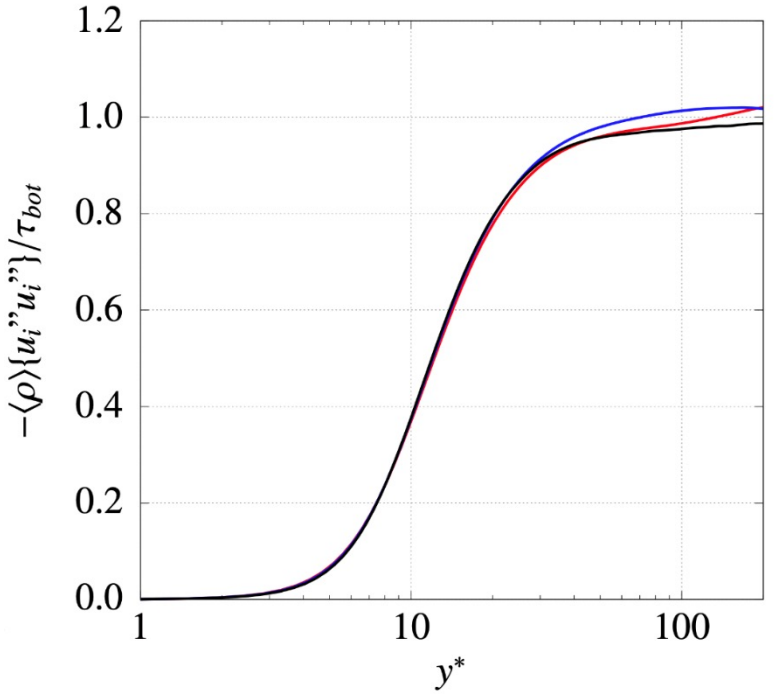


Velocity fluctuations and Reynolds stress



Bottom wall side

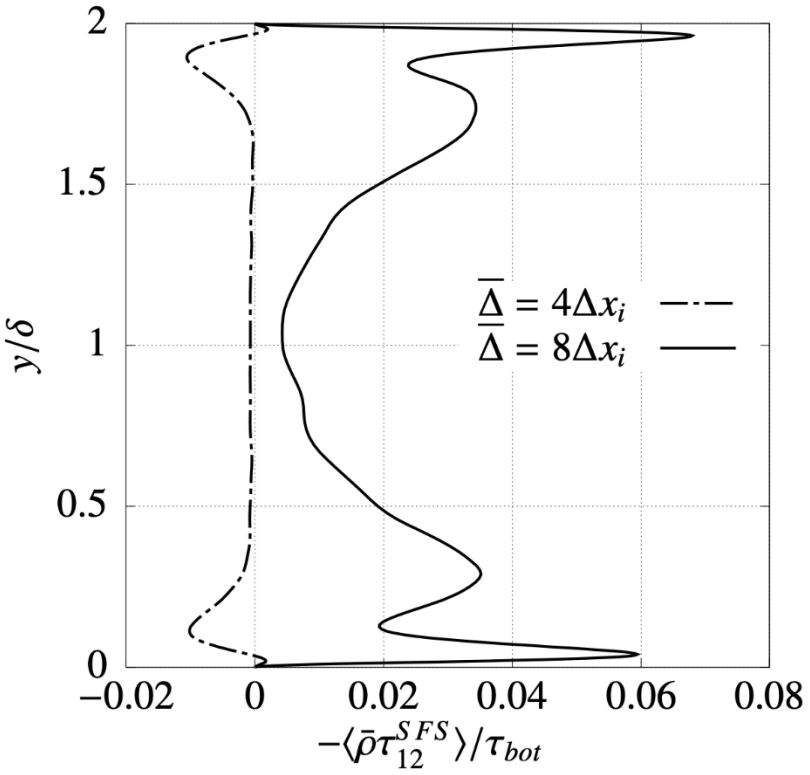
Top wall side

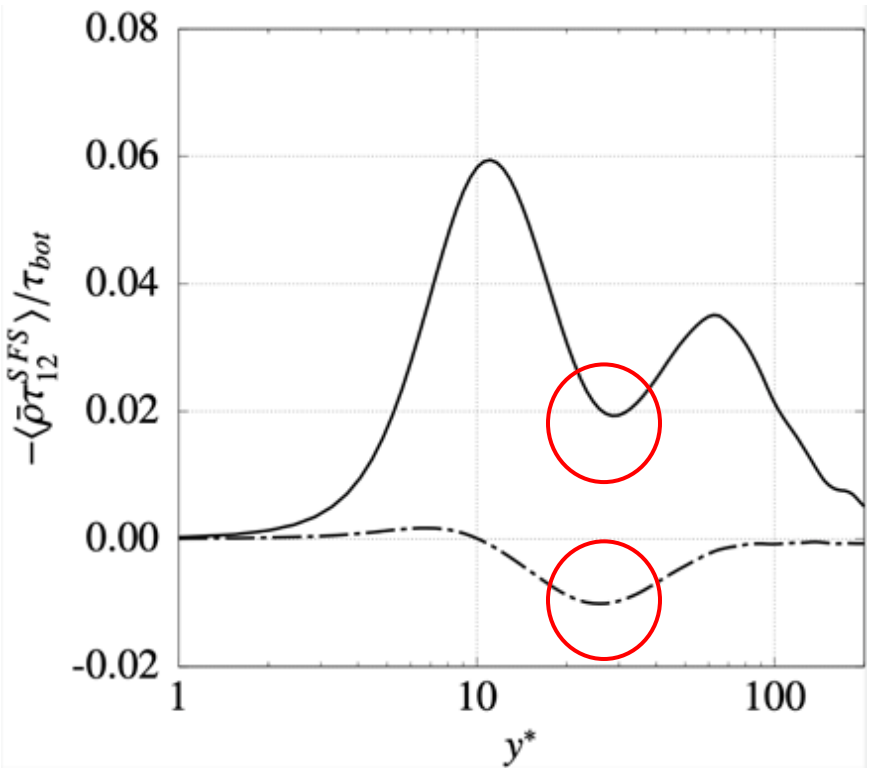


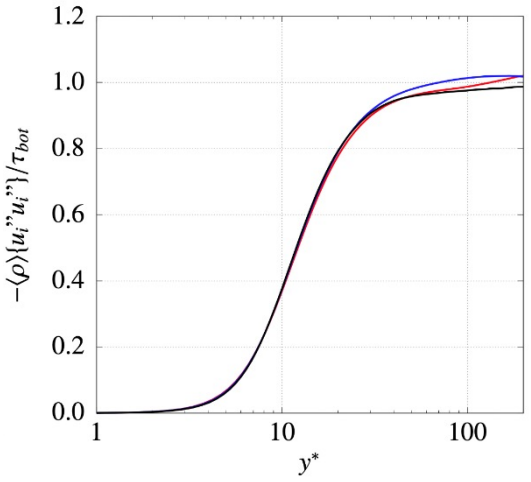
Reynolds stress in bottom wall side

- Velocity fluctuations and Reynolds stress have excellent collapses
  - Compressible effects on RANS terms are so small that semi-local scaling works
- Fluctuations are symmetric between the top and bottom wall sides.
  - We can focus on only the bottom wall side (only one side).

Averaged SFS stress profiles (M8-DNS)







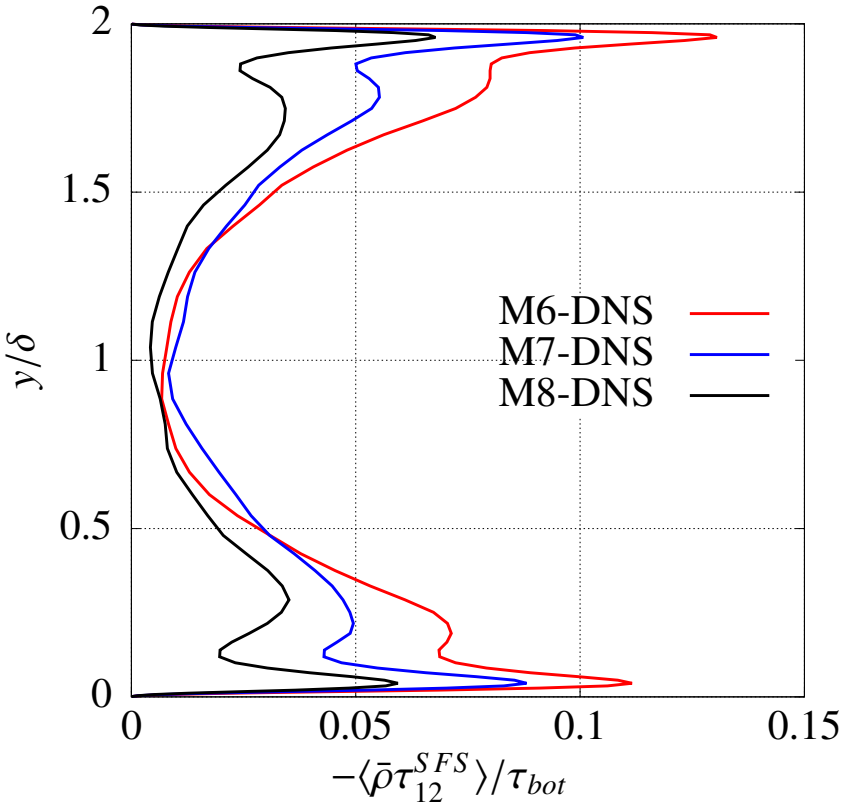
Reynolds stress

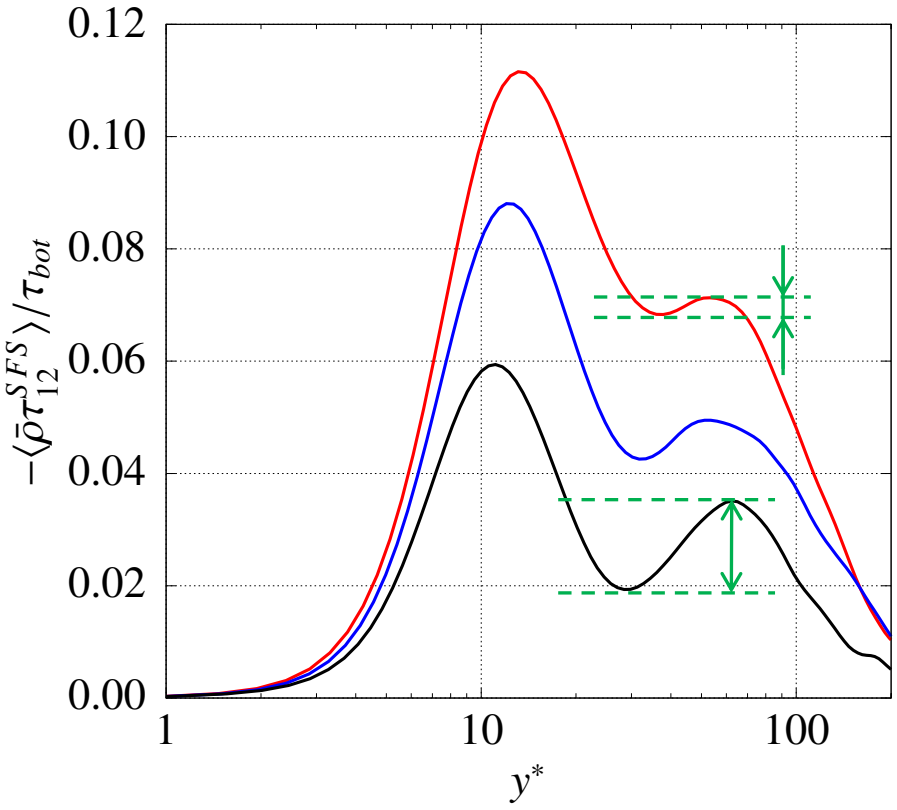
SFS stress: $\tau_{ij} = \widetilde{u_i u_j} - \tilde{u}_i \tilde{u}_j$

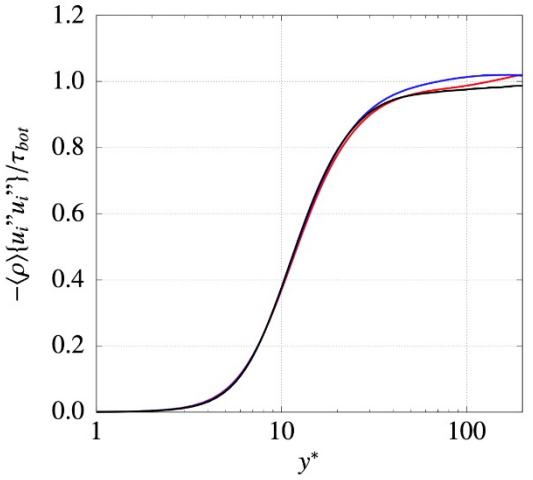
$\widetilde{(\cdot)}$: Favre spatial filter

- SFS stress with the weaker filter is negative in the entire domain.
  - ➢ Momentum transport in small scale is against Reynolds stress.
- SFS stress with the stronger filter has a deficit at the same location.
  - ➢ The deficit of the SFS stress is induced by small-scale turbulence

Effect of Mach number on SFS stress







Reynolds stress

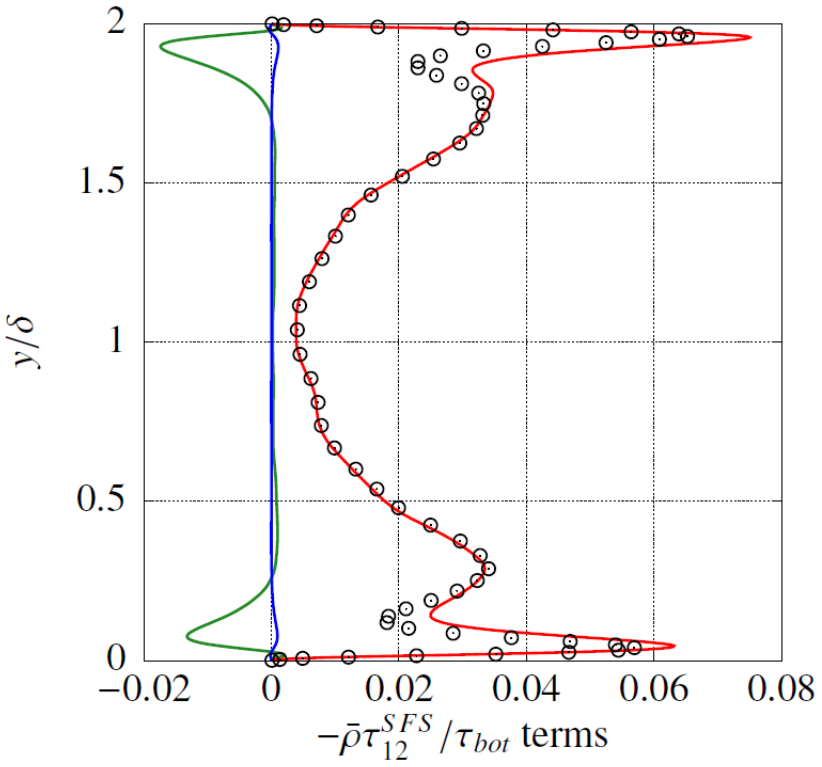
SFS stress: $\tau_{ij} = \widetilde{u_i u_j} - \tilde{u}_i \tilde{u}_j$

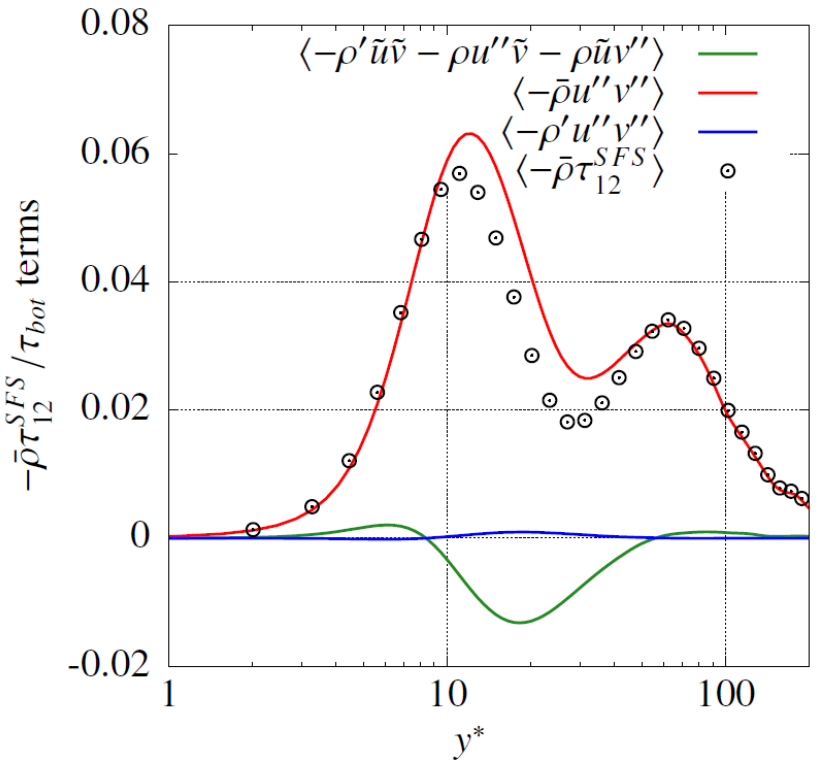
$\widetilde{(\cdot)}$: Favre spatial filter

$\langle\cdot\rangle$:averaging in (x, z) plane

- All cases have a deficit of the shear SFS stress around $y^* = 30$.
- The deficit becomes deeper with an increase in Mach number.
  - The deficit is associated with compressible effects.
  - We need to account for compressible effects even when semi-local scaling works.

Mathematical decomposition for SFS stress





Residual values:

$\phi' = \phi - \bar{\phi}$

$\phi'' = \phi - \tilde{\phi}$

$\overline{(\cdot)}$: Spatial filter

$\widetilde{(\cdot)}$: Favre spatial filter

The SFS stress can be decomposed to

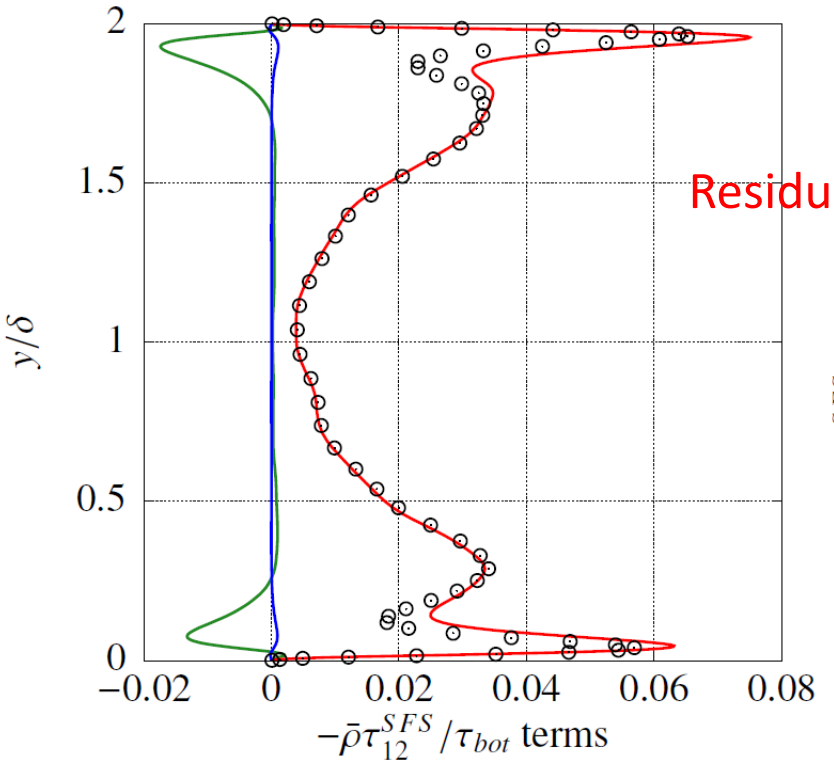
Residual velocity motions

$$-\langle \bar{\rho}\tau_{12}^{SFS} \rangle = -\langle \overline{\rho u v} \rangle + \langle \bar{\rho}\tilde{u}\tilde{v} \rangle = -\langle \rho'\tilde{u}\tilde{v} \rangle - \langle \rho u''\tilde{v} \rangle - \langle \rho\tilde{u}v'' \rangle - \langle \bar{\rho}u''v'' \rangle - \langle \rho' u''v'' \rangle$$

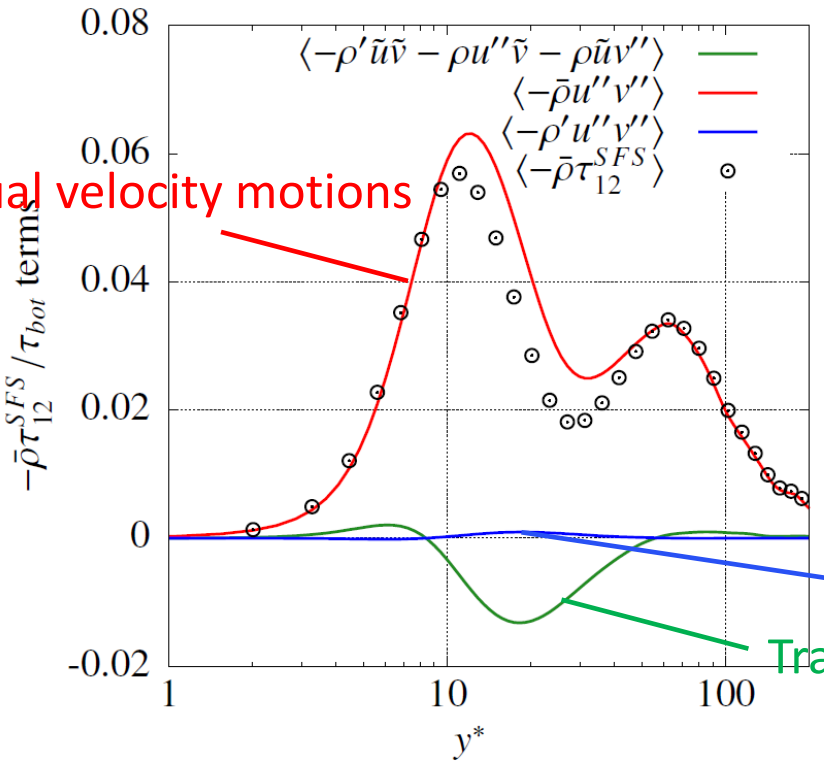
Transport by filtered flow

3rd-order correlation

Mathematical decomposition for SFS stress



Residual velocity motions



Residual values:

$\phi' = \phi - \bar{\phi}$

$\phi'' = \phi - \tilde{\phi}$

$\overline{(\cdot)}$: Spatial filter

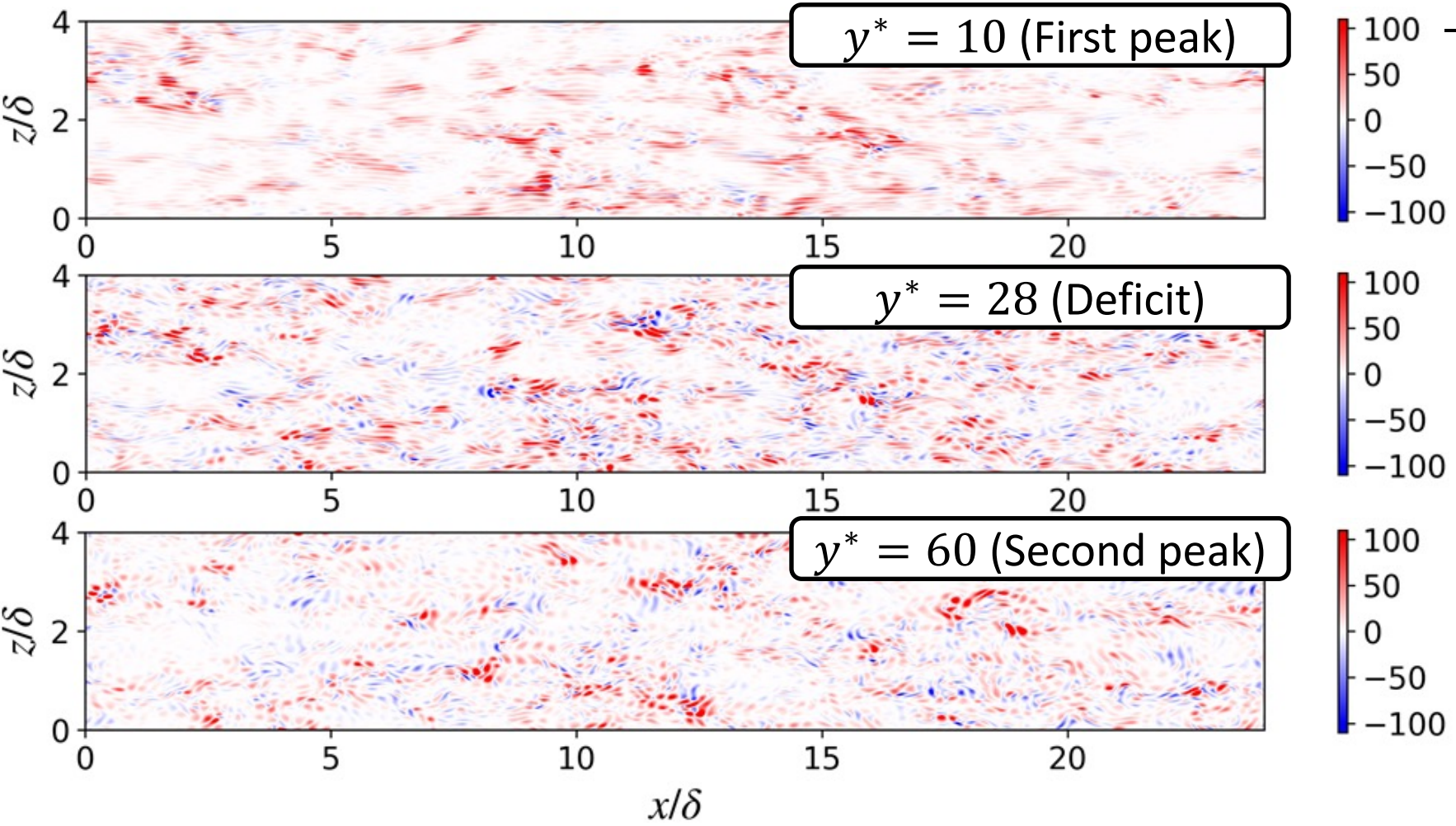
$\widetilde{(\cdot)}$: Favre spatial filter

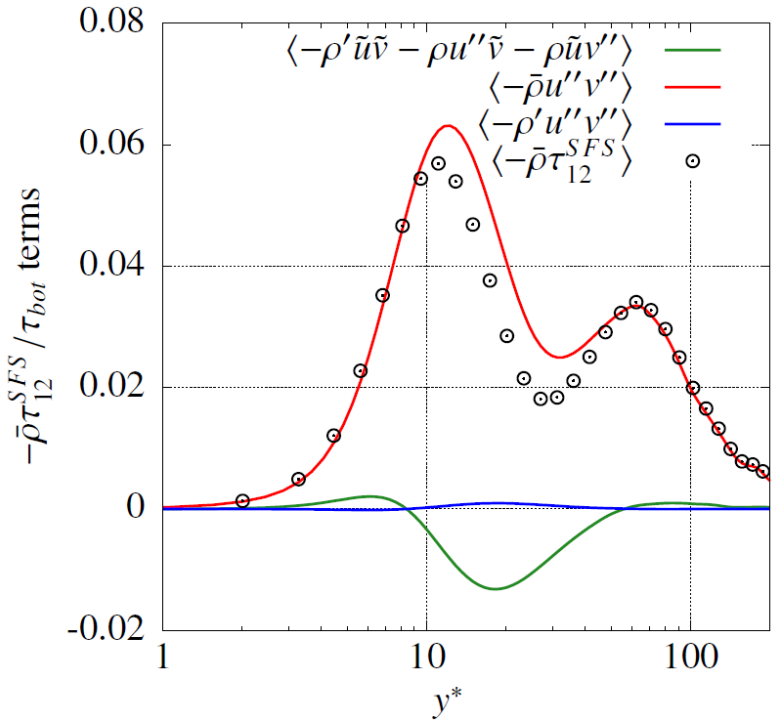
3rd-order correlation

Transport by filtered flow

- The contributions of the residual velocity motions are dominant.
- The profile of the residual velocity motions agree with the SFS stress.
  - The deficit of the shear SFS stress is caused by the residual velocity motions.
  - The flow dynamics regarding residual velocity should be examined.

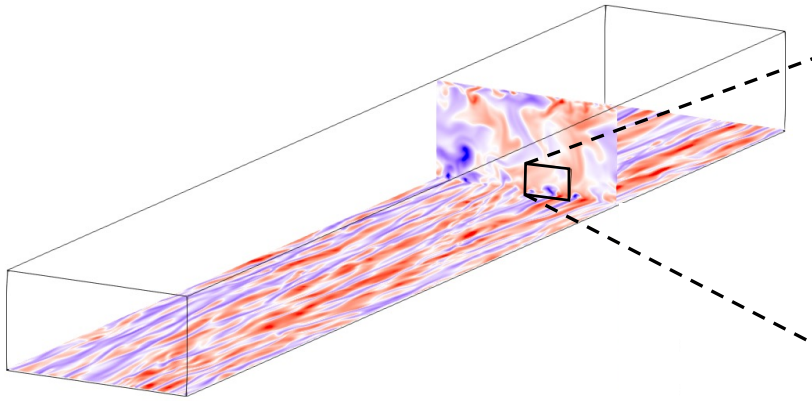
Visualization of residual velocity contributions



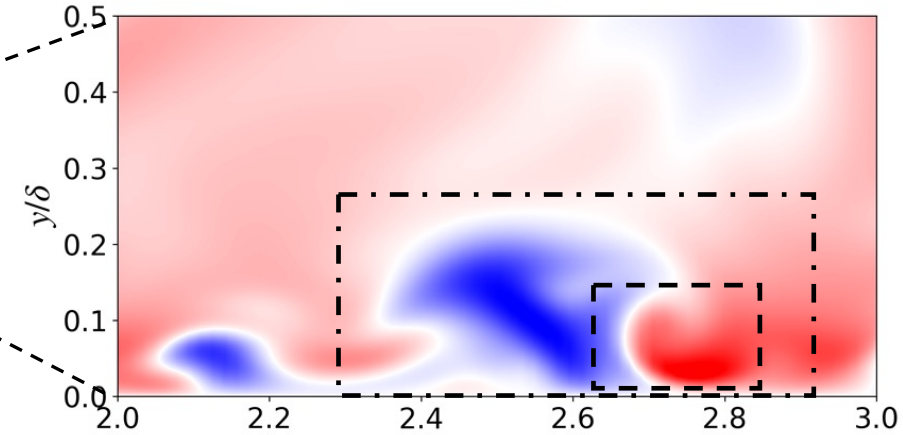


- Structures are patchy and negative contributions are observed at $y^* = 28$ and 60.
  - ➢ Why are the negative contributions enhanced around $y^* = 28$?

Flow field in cross-stream plane



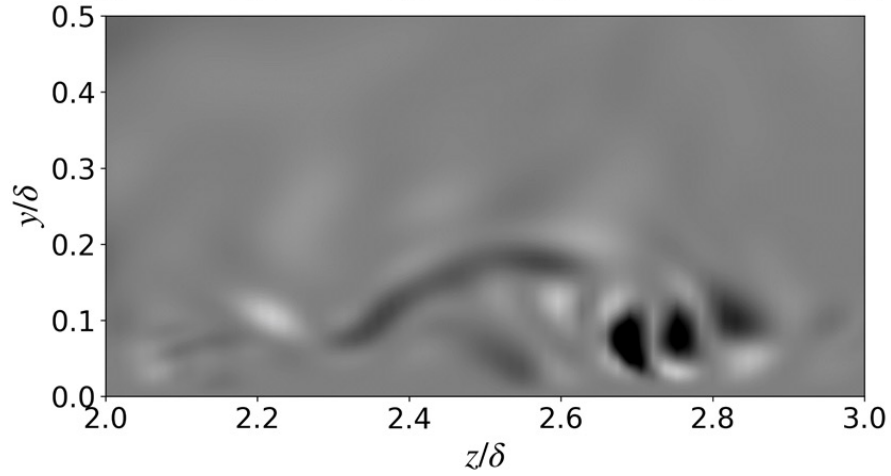
M8-DNS



$u''\ (\mathrm{m}\cdot\mathrm{s}^{-1})$

$u'' = u - \{u\}$

$\{\cdot\}$: Favre average



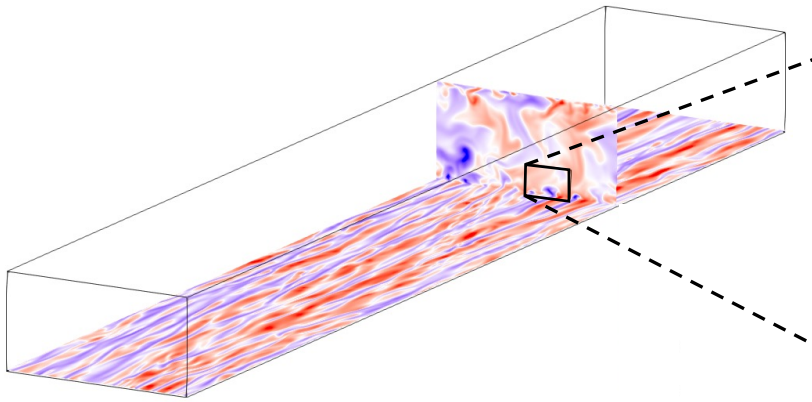
$-\bar{\rho}u''v''(\mathrm{Pa})$

$\phi'' = \phi - \tilde{\phi}$

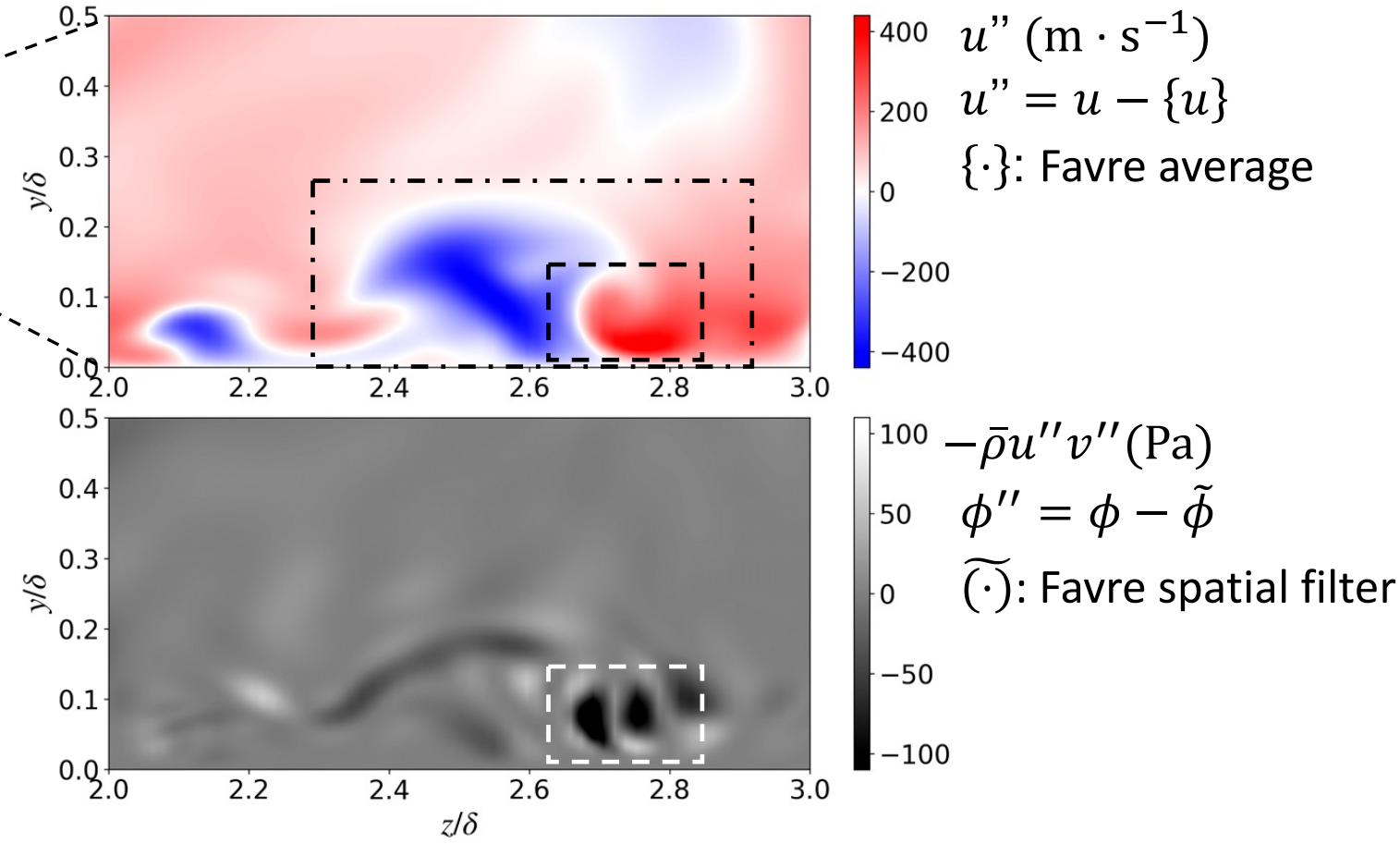
$\widetilde{(\cdot)}$: Favre spatial filter

- The low-speed streak expands in the wall-normal direction.
  - Low-temperature is heated and volume expansion occurs.
- The high-speed streak is entrained under the low speed-streak.

Flow field in cross-stream plane



M8-DNS



$u''\ (\mathrm{m}\cdot\mathrm{s}^{-1})$

$u'' = u - \{u\}$

$\{\cdot\}$: Favre average

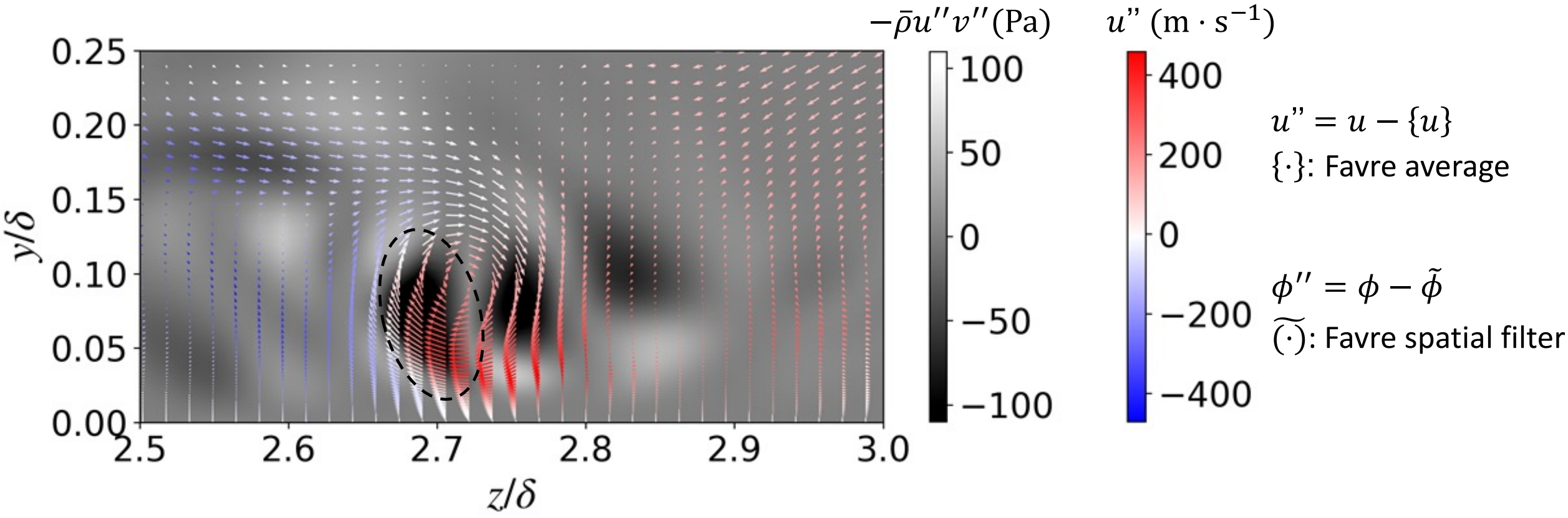
$-\bar{\rho}u''v''(\mathrm{Pa})$

$\phi'' = \phi - \tilde{\phi}$

$\widetilde{(\cdot)}$: Favre spatial filter

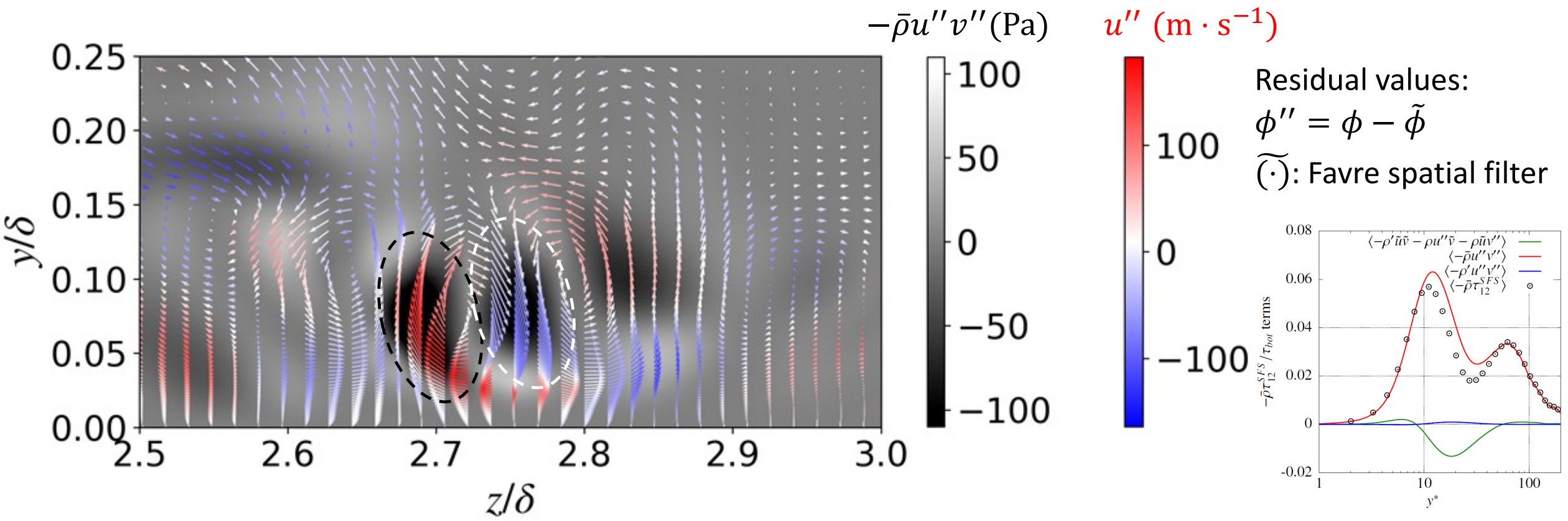
- The $-\bar{\rho}u''v''$ has strong negative patchy structure.
- The patchy structure is observed in the high-speed streak.
  - ➢ Flow dynamics in the high-speed streak is the key for the deficit of the shear SFS.

Flow field in cross-stream plane



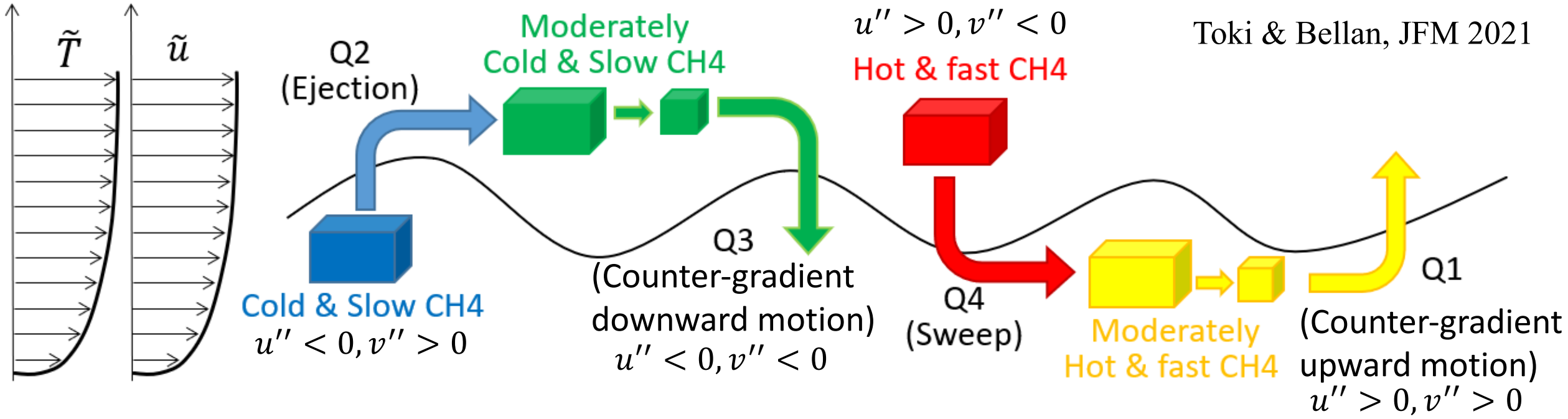
- Part of the high-speed streak is rolled up by the upward motion.
  - ➢ This motion should induce counter-gradient momentum flux.
- This phenomenon occurs at the interface between high-speed and low-speed streaks.
  - ➢ Is its scale sufficiently small to be removed by the spatial filter?

Flow field in cross-stream plane



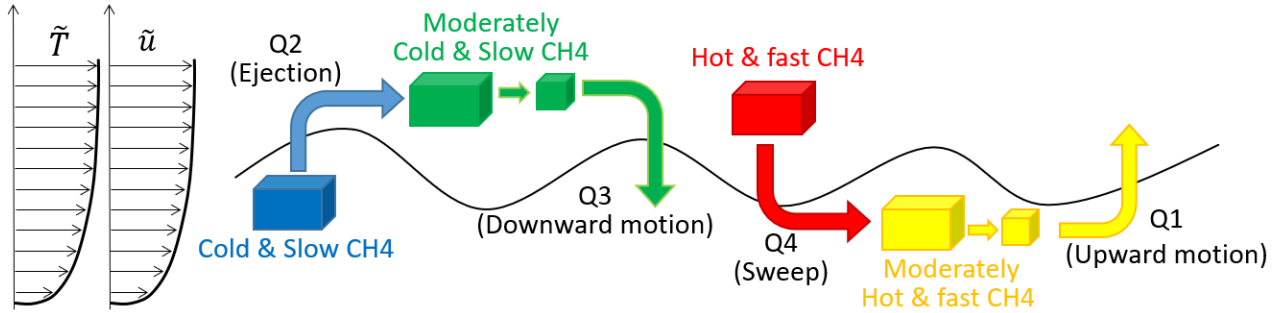
- Upward motion of the high-speed residual velocity is removed by the spatial filter.
- The SFS acts to compensate for the missing contribution.
  - ➢ The upward motion induces a negative contribution to the SFS stress.
- The downward motion of the low-speed residual velocity is also removed.

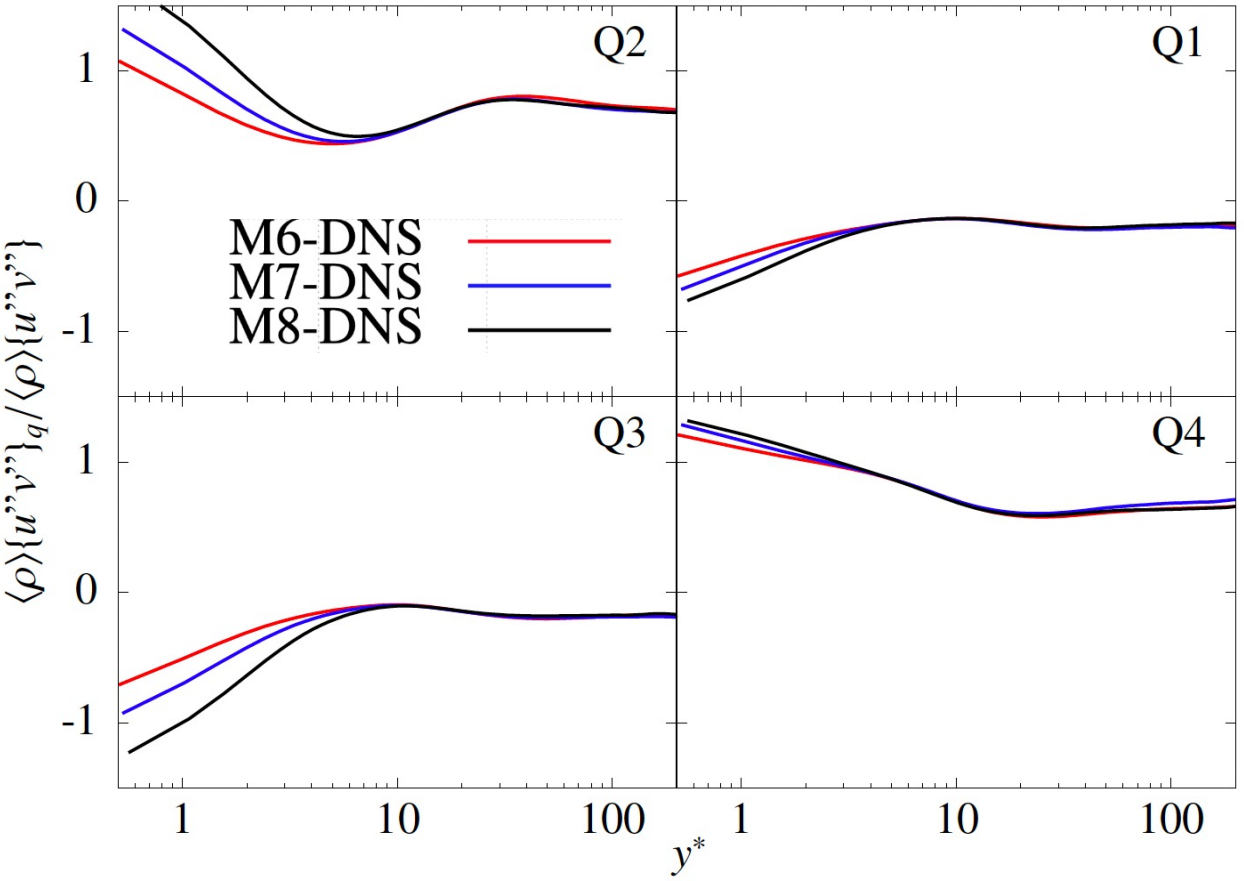
Quadrant analysis

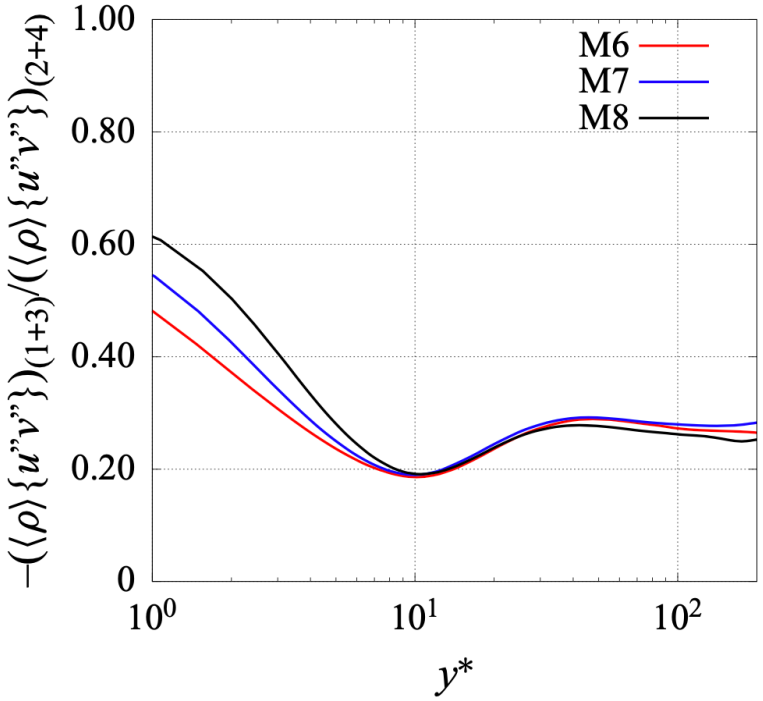


- Velocity and temperature profiles monotonically increase from the wall.
- Cold ($T'' < 0$) and slow ($u'' < 0$) fluids tend to be correlated with upward motion ($v'' < 0$), and vice versa.
  - ➢ Generally, contributions of Q2 (ejection) and Q4 (sweep) are dominant.

Quadrant analysis for Reynolds shear stress



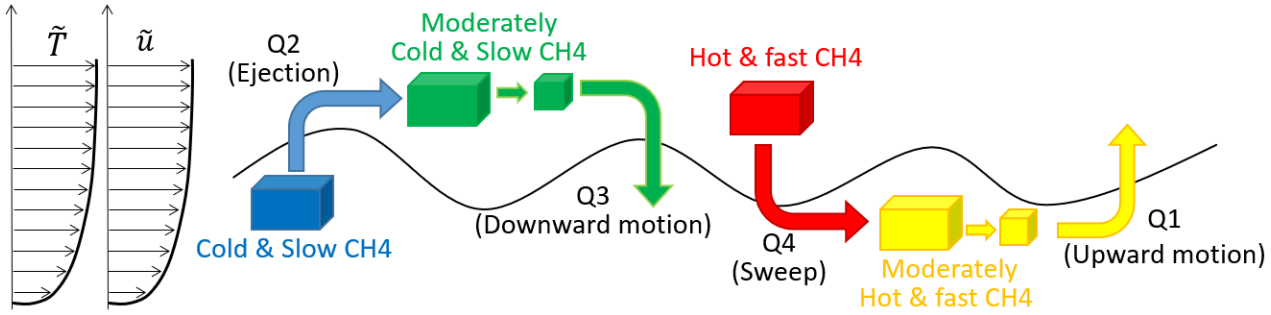


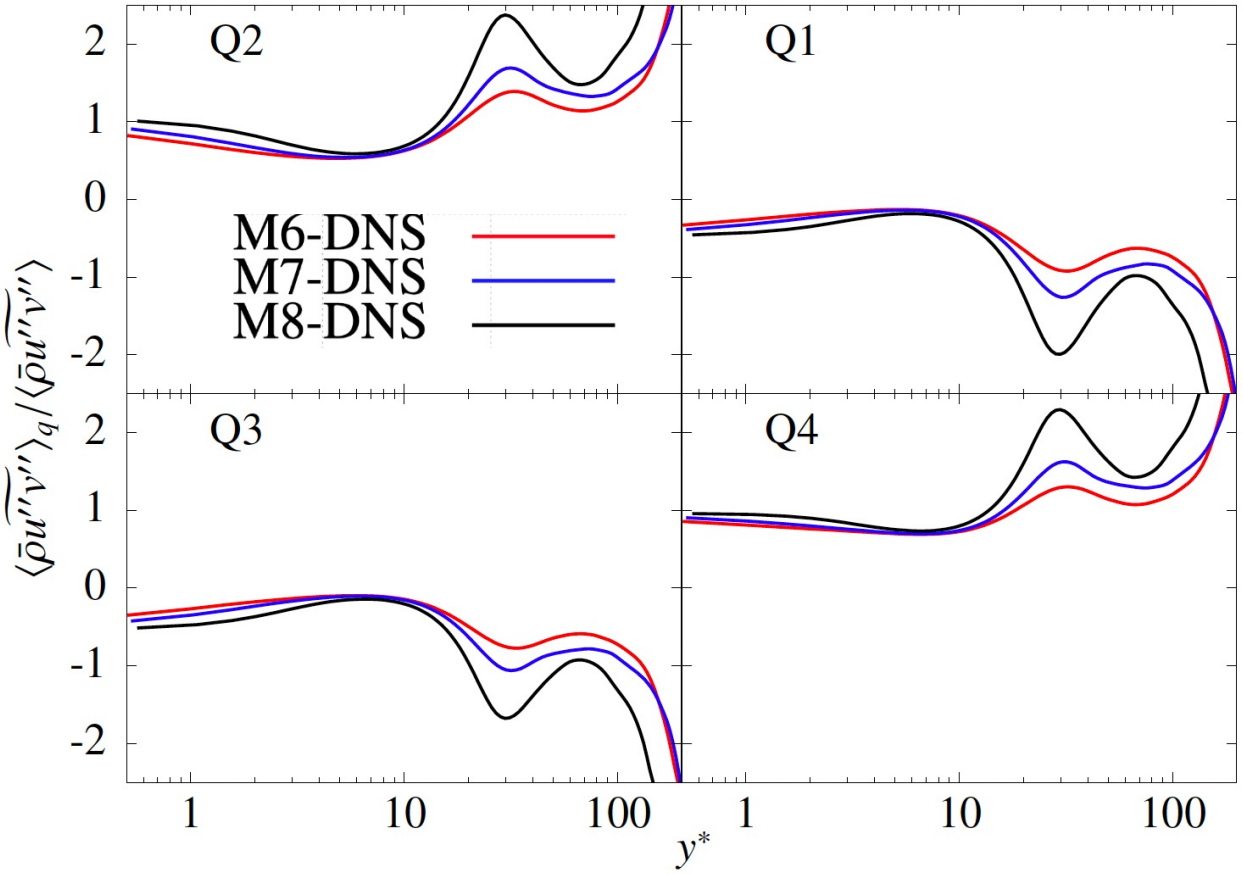


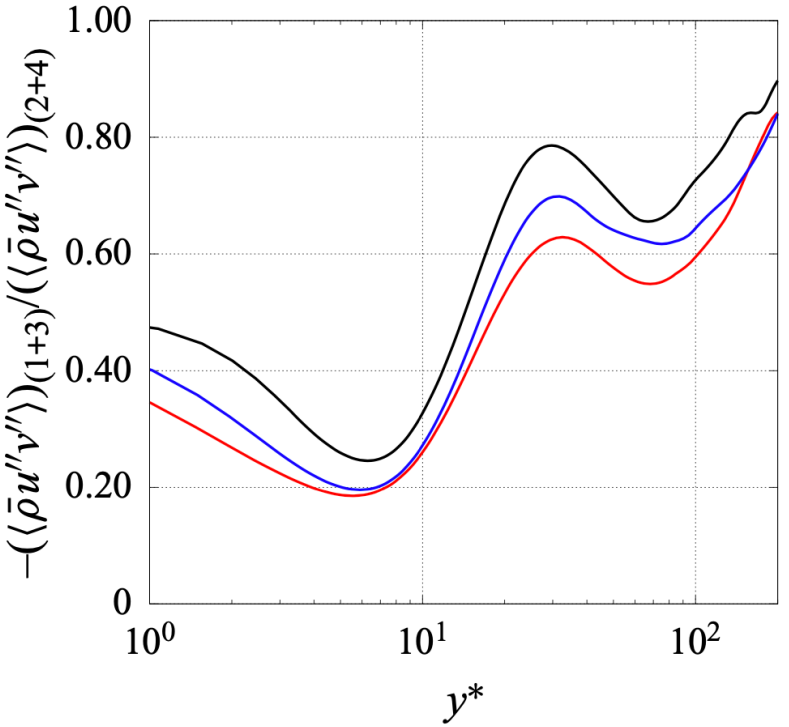
Ratio for the sum of the Q1 and Q3 contributions and that of the Q2 and Q4 motion.

- Q2 and Q4 events are dominant
- Only 30% of momentum is counteracted by Q1 and Q3 events in the Reynolds stress.

Quadrant analysis for residual contributions



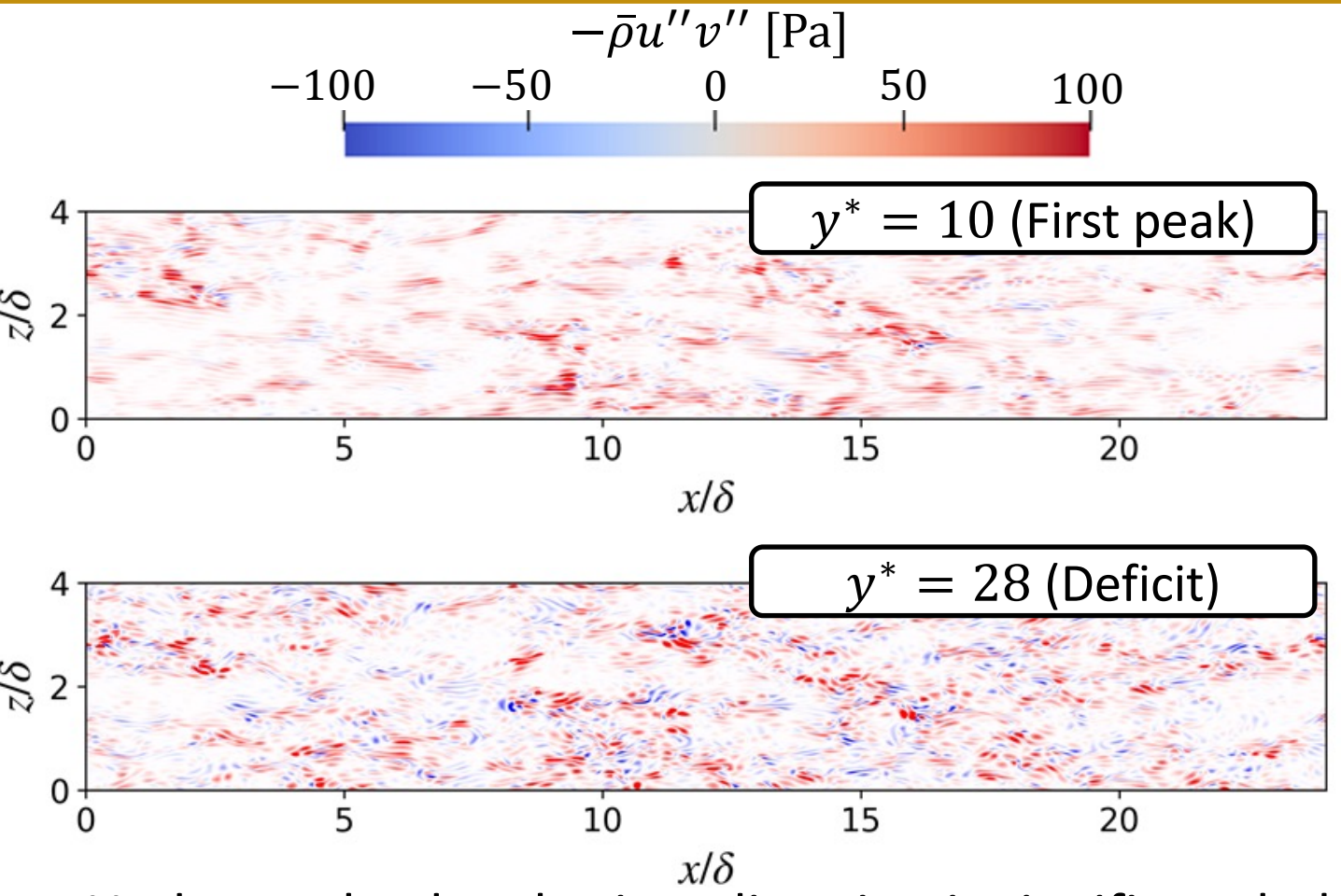


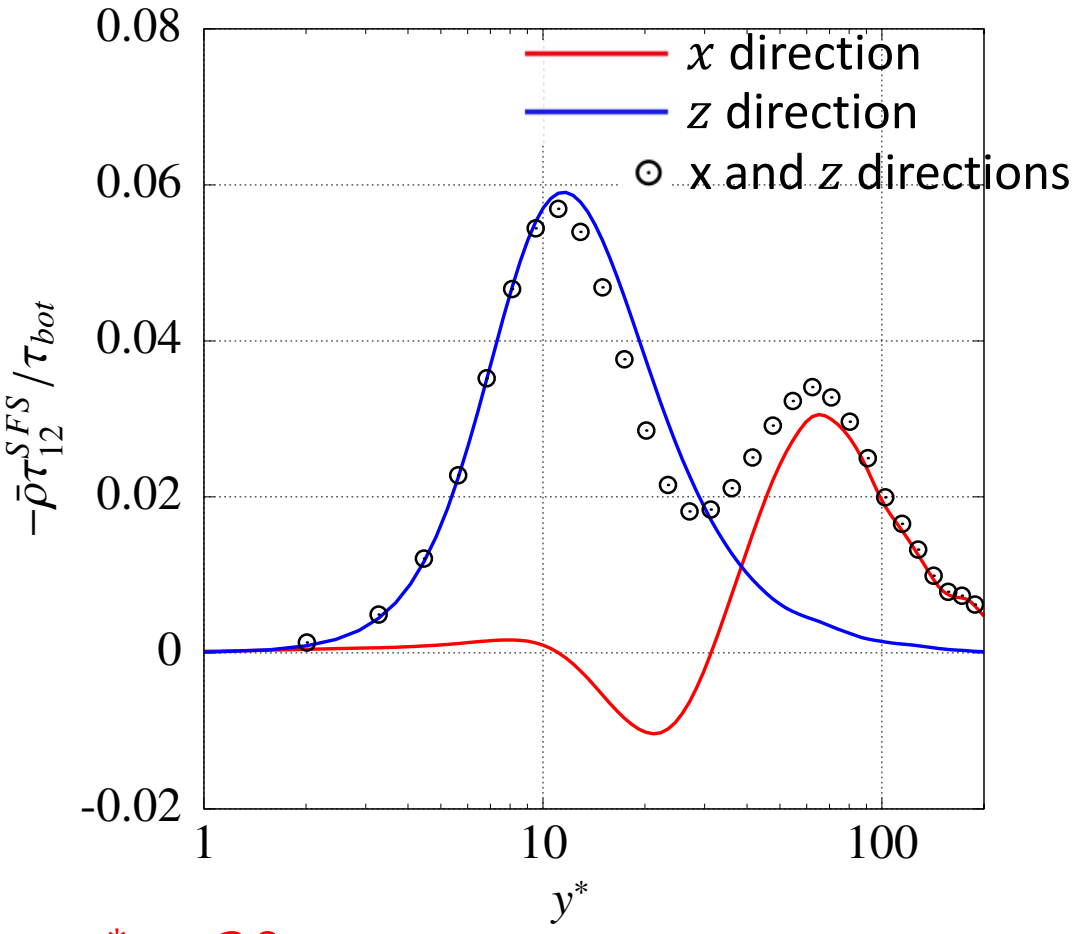


- Q2 and Q4 events are dominant
- Q1 and Q3 events are pronounced around $y^* = 30$.
- Nearly 80% the momentum is counteracted at Mach 8 case.

➢ Q1 and Q3 events induce the SFS deficit.

Effects of filter direction

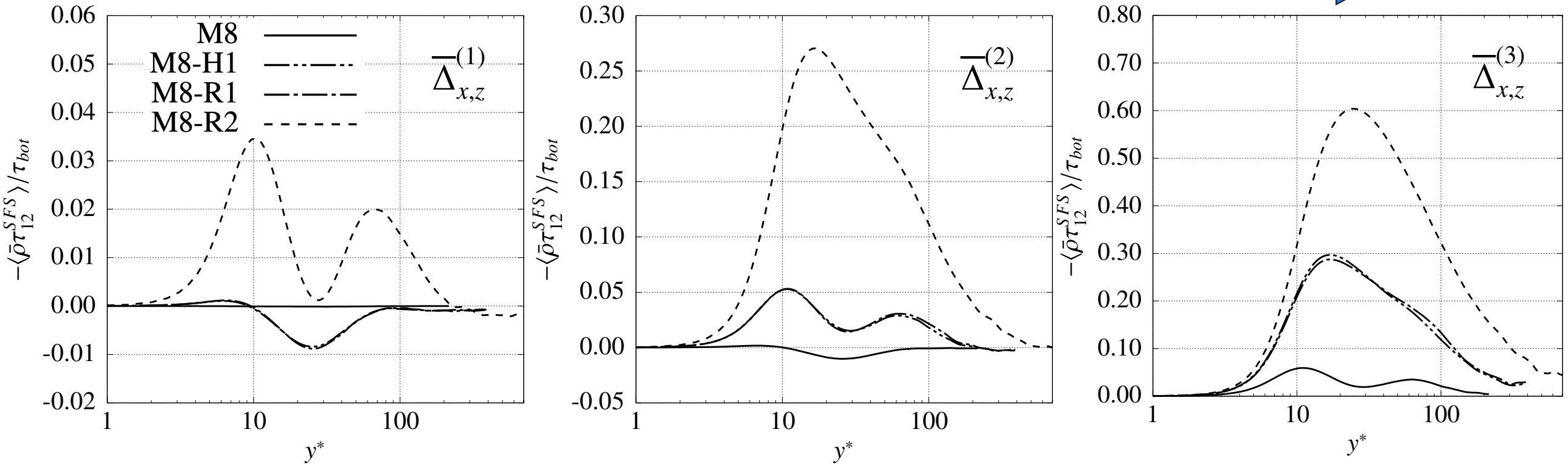




- Underresolved scales in z direction is significant below $y^* = 20$
- Those in x direction have negative value around $y^* = 20$ and become dominant over $y^* = 30$
  - ➢ The deficit of the SFS shear stress is driven by SFS activity in x direction

Effects of Reynolds number

Strength of filter



M8: $Re_\tau^* = 213$

M8-H1(larger δ): $Re_\tau^* = 385$

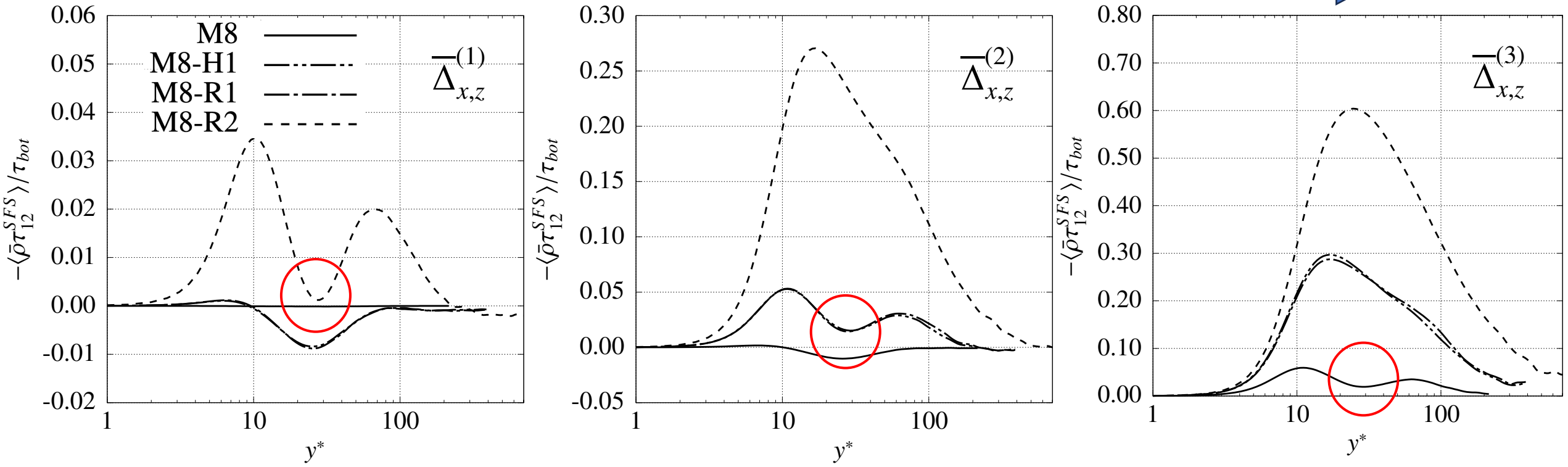
M8-R1(larger ρ): $Re_\tau^* = 384$

M8-R2(larger ρ): $Re_\tau^* = 698$

Increasing Reynolds number

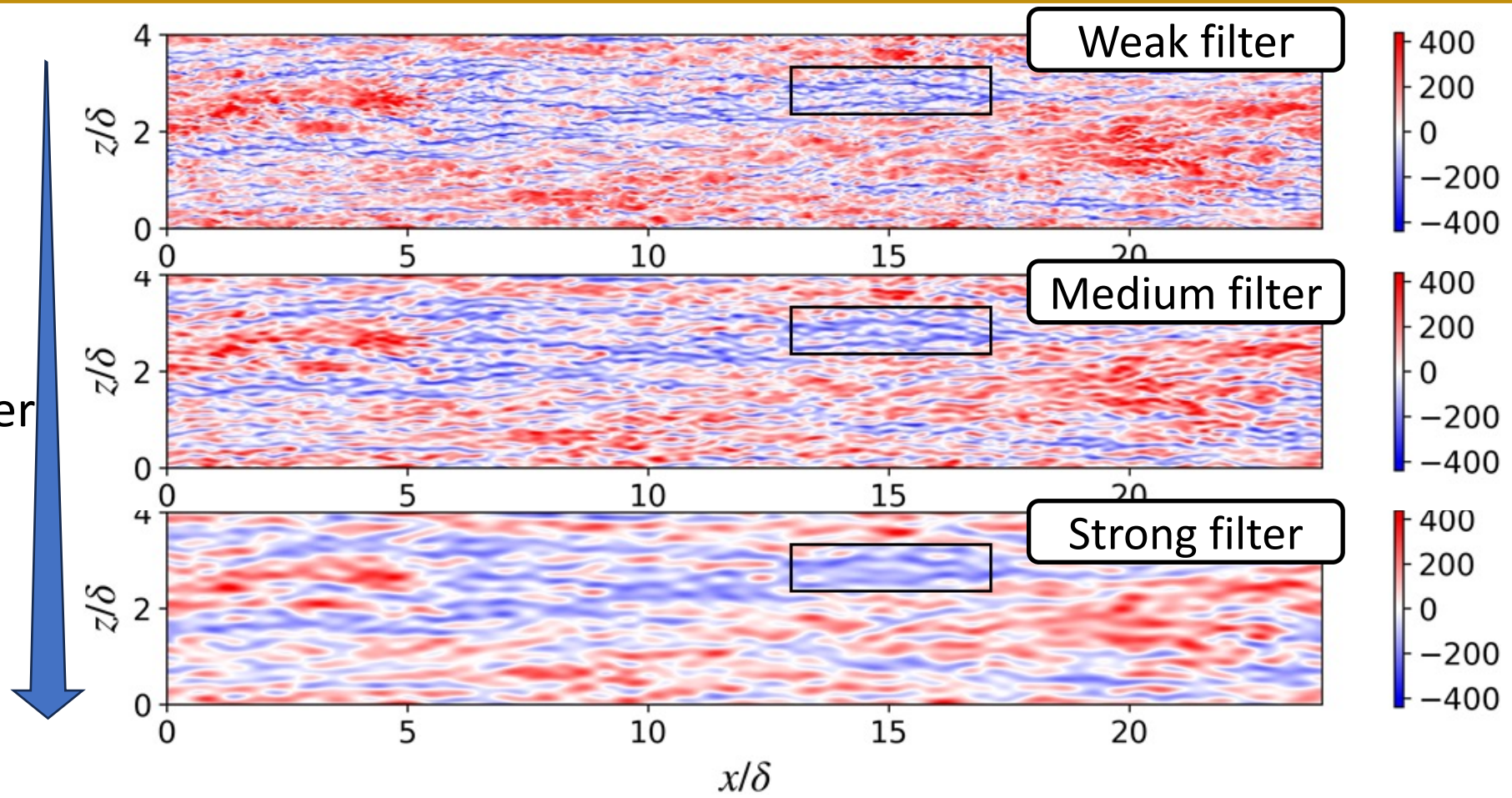
Effects of Reynolds number

Strength of filter



- The SFS shear stress deficit appears at any Reynolds number with a certain filter.
- The deficit disappears when a strong filter is applied to high Reynolds number cases.
  - ➢ Do LES models need to account for the deficit?

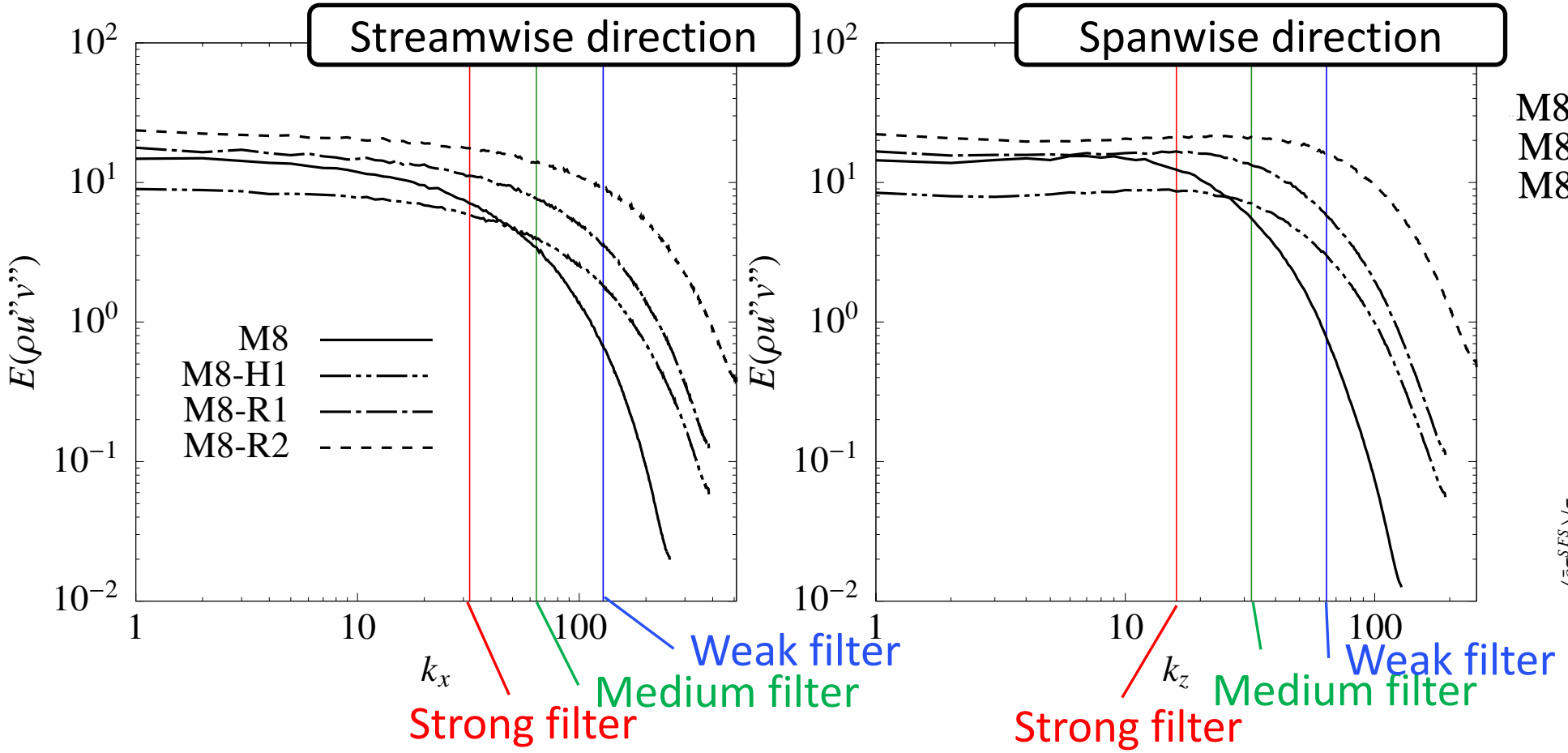
Effects of filtering (Highest Re_τ^* at $y^* = 26$)

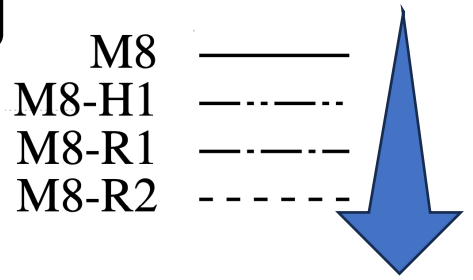


Strength of filter

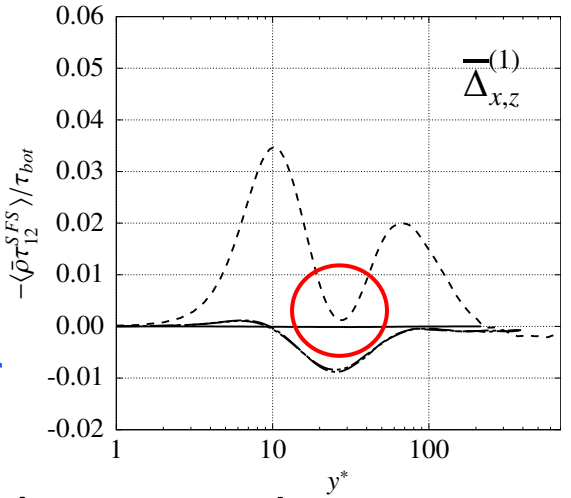
- Fine streaks are observed in the black rectangle box for the weak filter
- The structures get weakened and disappear with a stronger filter.
  - Strong filters have the potential to remove important structures.

Spectra of Reynolds stress at $y^* = 25$





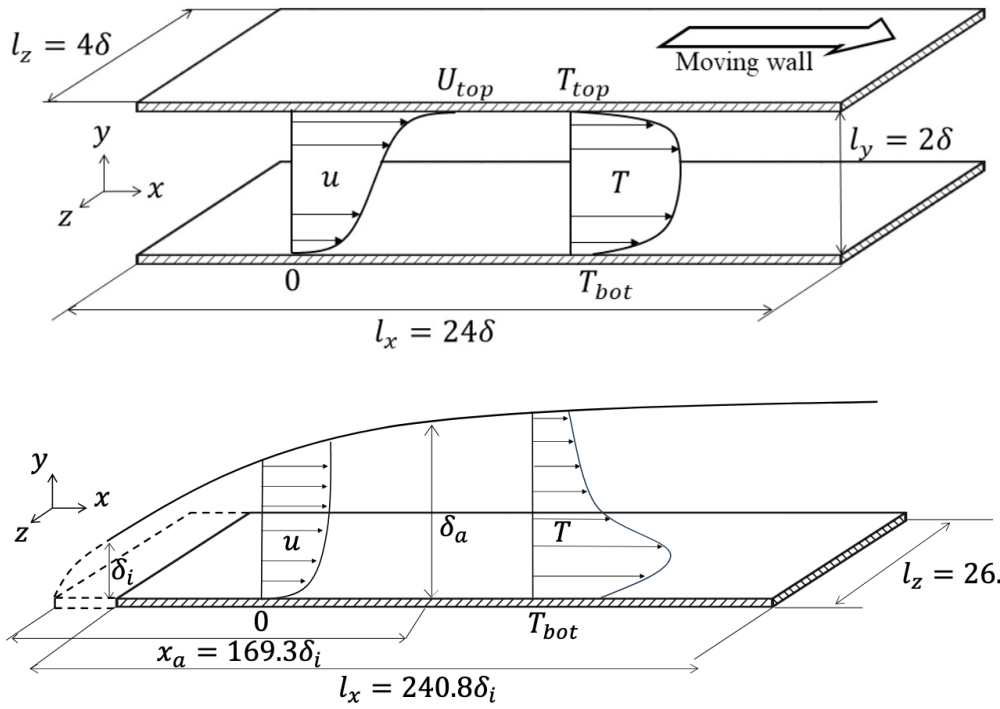
Increasing Re_τ^*

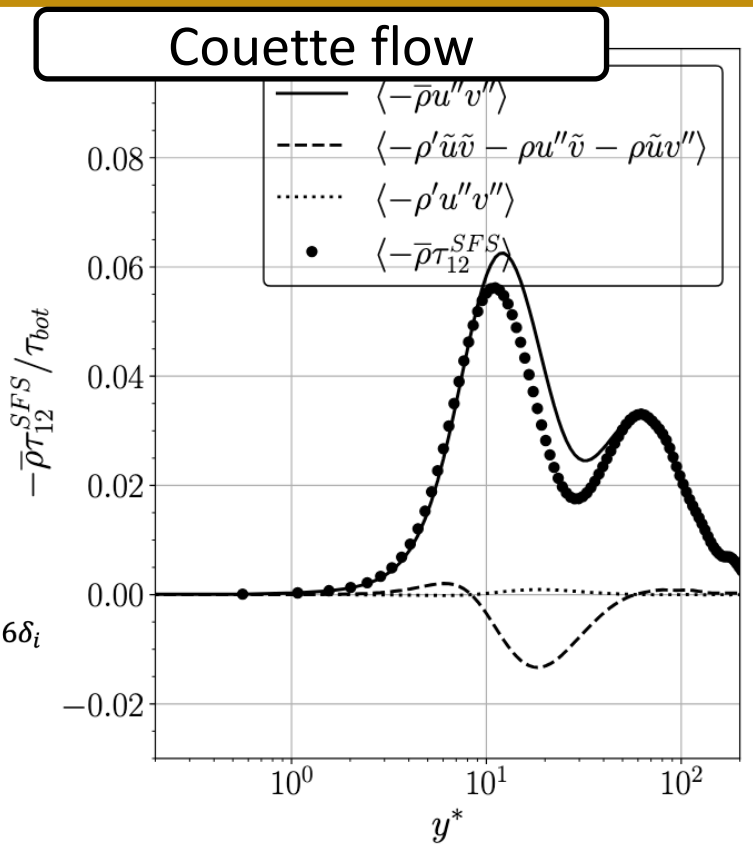


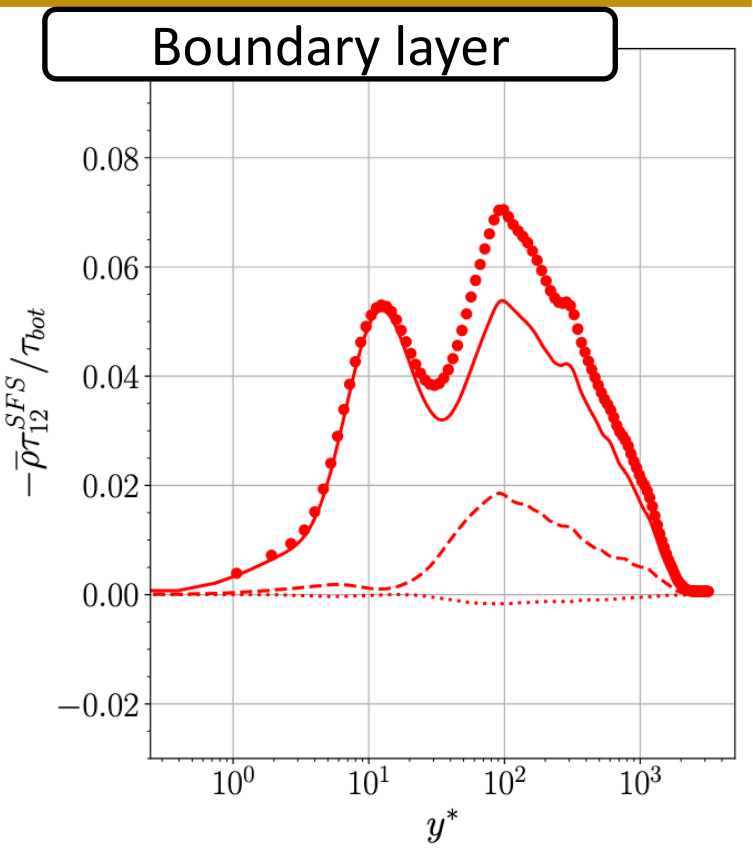
- The cut-off wave numbers need to be lower than the beginning of the cascade.
- When a reasonable filter is applied, the SFS deficit is always observed.
  - ➢ The deficit of SFS shear stress is significant for any Reynolds number.

Ongoing and Future Work

Comparison between boundary layer and Couette



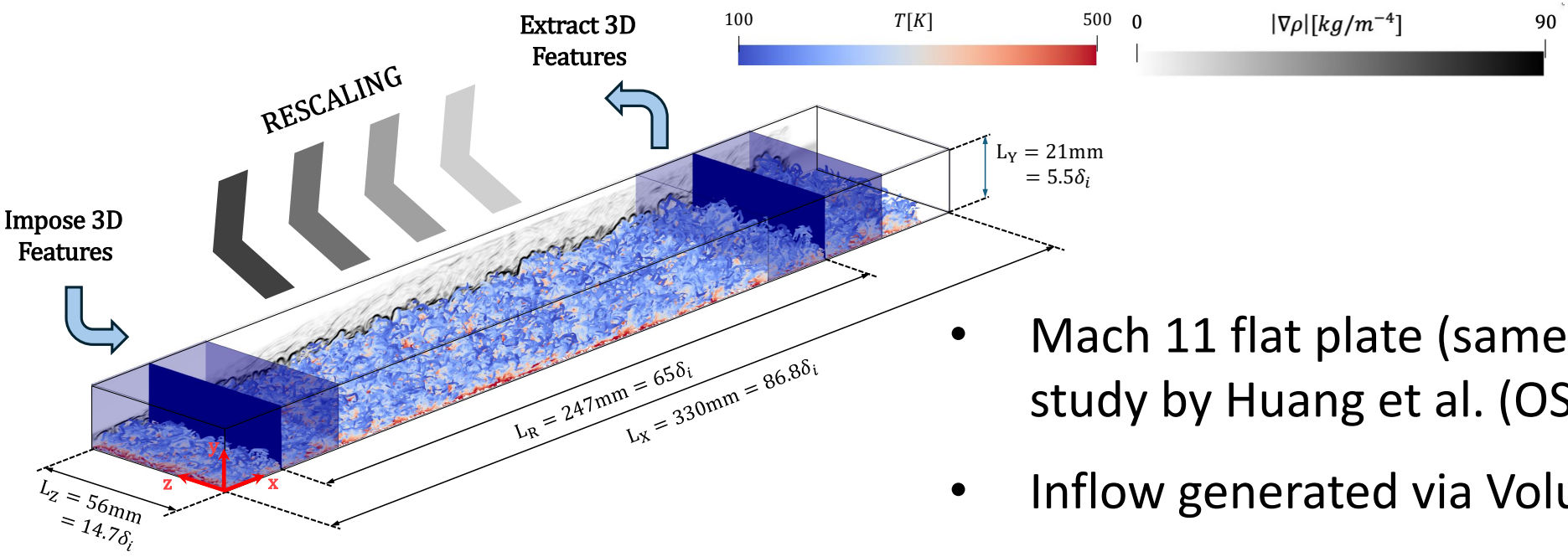




- The SFS shear stress deficit is observable in the hypersonic boundary layer.
  - ➢ Internal flow can be used to discuss wall-bounded turbulence.

A posteriori LES of a hypersonic boundary layer

PURDUE UNIVERSITY

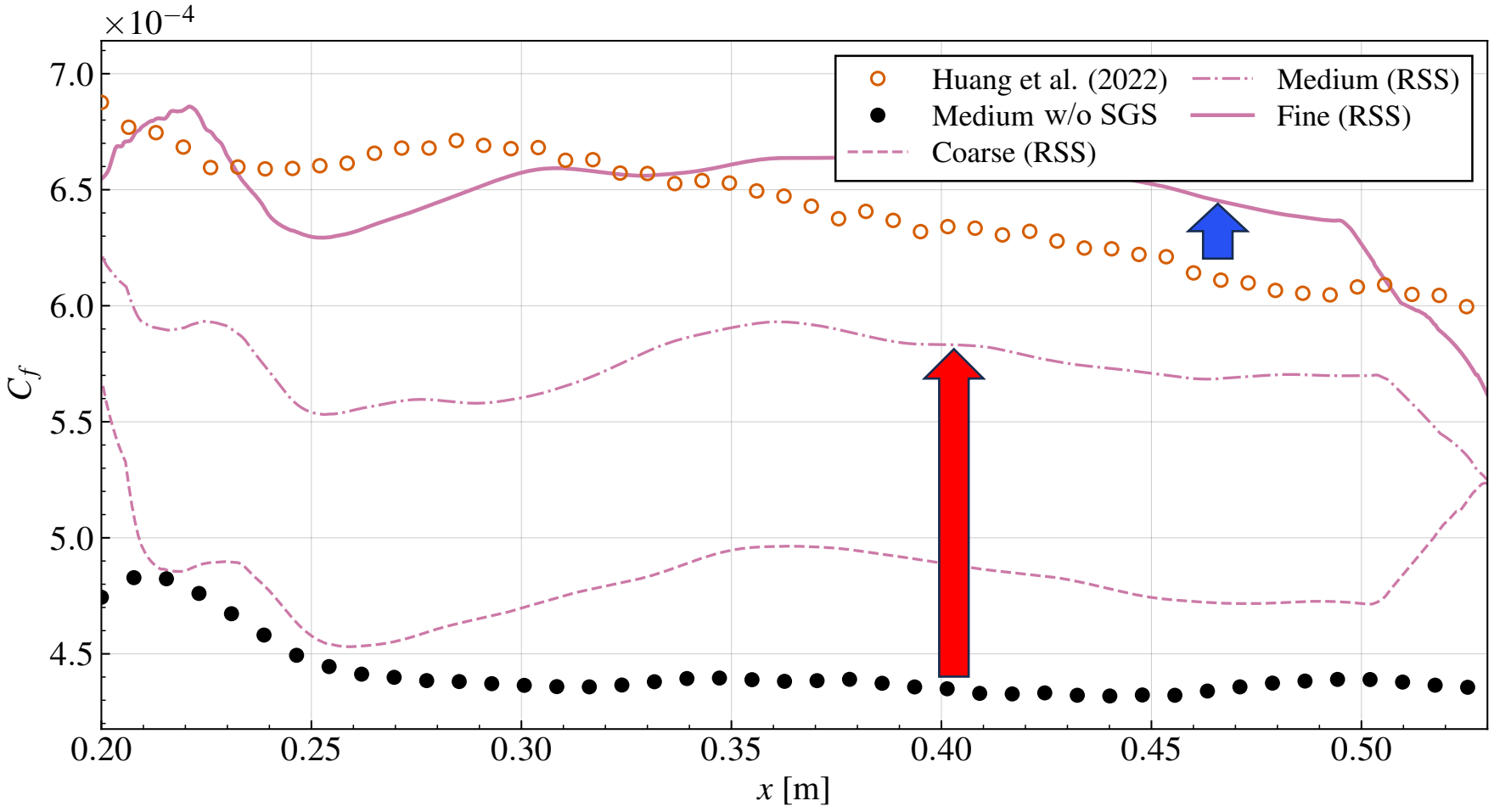


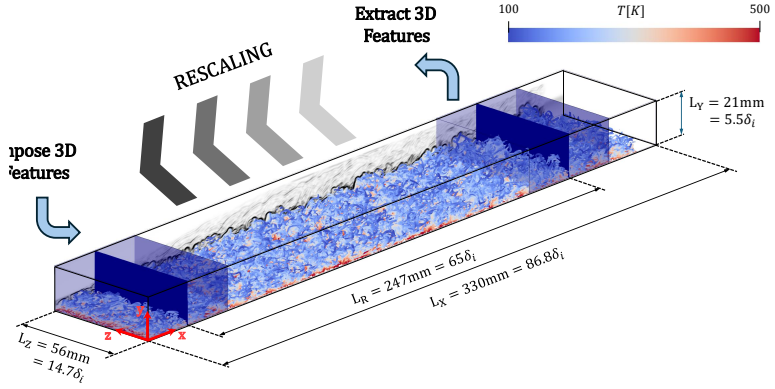
- Mach 11 flat plate (same conditions as the DNS study by Huang et al. (OSU), JFM 2022)
- Inflow generated via Volumetric rescaling[2].

Grid	Δx^+_{LES}	$\frac{\Delta x^+_{LES}}{\Delta x^+_{DNS}}$	N_x	Δz^+_{LES}	$\frac{\Delta z^+_{LES}}{\Delta z^+_{DNS}}$	N_z	$\Delta y^+_{LES,min}$	$\frac{\Delta y^+_{LES,min}}{\Delta y^+_{DNS,min}}$	N_y
Coarse	66.3	9.34	432	50.7	7.68	92	1.36	3.16	112
Medium	44.9	6.33	640	33.79	5.12	144	1.02	2.37	144
Fine	29.96	4.22	960	22.51	3.41	216	0.76	1.76	192

2. Takahiko Toki, Victor C.B. Sousa, Yongkai Chen, Giannino Ponchio Camillo, Alexander Wagner, and Carlo Scalo, "Large-eddy simulations of conical hypersonic turbulent boundary layers over cooled walls via volumetric rescaling method," *Journal of Fluid Mechanics*, Vol. 1003, A28, 2025.

A posteriori LES of a hypersonic boundary layer





(1) RSS-LES predicts wall shear stress more accurately than implicit LES on the medium mesh.

(2) RSS-LES overpredicts wall shear stress on the fine mesh.

Conclusion

Conclusion

PURDUE UNIVERSITY

LES of a hypersonic conical boundary layer at Mach 7.4.

- ❑ Hypersonic LES can be used to discuss unsteadiness qualitatively.
- ❑ Predicted wall heat flux largely varies with the mesh refinement.
- ❑ Fluctuations of velocity and temperature show grid-dependency only near the wall.
- ❑ An understanding of the near-wall turbulence is important to improve LES models.

DNS of hypersonic Couette flows at Mach 6, 7, and 8.

- ❑ Semi-local scaling works well with velocity fluctuations and Reynolds stresses
- ❑ The SFS shear stress has a deficit, and it becomes deeper with an increase in Mach number.
- ❑ The deficit of the SFS shear stress is induced by the counter-gradient type motions of the residual velocity.
- ❑ We need to account for compressible effects in large eddy simulations of hypersonic wall-bounded flows, even when semi-local scaling works with Reynolds-averaged turbulent statistics.

Acknowledgement

Advisor: Carlo Scalo

Collaborators: Victor Sousa, Yongkai Chen, Giannino Ponchio Camillo, Alexander Wagner

Funding:

This work was supported by the Office of Naval Research (ONR) under grants N00014-21-1-2475 and N00014-23-1-2560.

Thank you!